*Review*

# Recent Breakthroughs in the Conversion of Ethanol to Butadiene

**Guillaume Pomalaza [1], Mickaël Capron [1], Vitaly Ordomsky [1,2] and Franck Dumeignil [1,*]**

[1] University Lille, CNRS, Centrale Lille, ENSCL, University Artois, UMR 8181-UCCS-Unité de Catalyse et Chimie du Solide, F-59000 Lille, France; pomalaza.g@gmail.com (G.P.); mickael.capron@univ-lille1.fr (M.C.); italy.Ordomsky@univ-lille1.fr (V.O.)

[2] Eco-Efficient Products and Processes Laboratory (E2P2L), UMI 3464 CNRS-Solvay, Shanghai 201108, China

[*] Correspondence: franck.dumeignil@univ-lille1.fr; Tel.: +33-(0)3-20-43-45-38

**Abstract:** 1,3-Butadiene is traditionally produced as a byproduct of ethylene production from steam crackers. What is unusual is that the alternative production route for this important commodity chemical via ethanol was developed a long time ago, before World War II. Currently, there is a renewed interest in the production of butadiene from biomass due to the general trend to replace oil in the chemical industry. This review describes the recent progress in the production of butadiene from ethanol (ETB) by one or two-step process through intermediate production of acetaldehyde with an emphasis on the new catalytic systems. The different catalysts for butadiene production are compared in terms of structure-catalytic performance relationship, highlighting the key issues and requirements for future developments. The main difficulty in this process is that basic, acid and redox properties have to be combined in one single catalyst for the reactions of condensation, dehydration and hydrogenation. Magnesium and zirconium-based catalysts in the form of oxides or recently proposed silicates and zeolites promoted by metals are prevailing for butadiene synthesis with the highest selectivity of 70% at high ethanol conversion. The major challenge for further application of the process is to increase the butadiene productivity and to enhance the catalyst lifetime by suppression of coke deposition with preservation of active sites.

**Keywords:** butadiene; ethanol; acetaldehyde; ETB; condensation; catalyst; oxide

## 1. Introduction

### 1.1. Scope of the Review

1,3-butadiene (butadiene, BD or $C_4H_6$) is essential to the production of numerous elastomers, such as styrene-butadiene rubber, polybutadiene, acrylonitrile-butadiene-styrene and others [1–3]. It is also used as a reagent in organic chemistry, particularly in Diels-Alder reaction [2]. At present, butadiene is predominantly extracted from the C4 steam cracker fractions [2]. Because the butadiene yield depends largely on the nature of the feedstock of the steam cracker, butadiene production is susceptible to market instability or trends in the petroleum industry, notably the emergent use of shale gas, which may lead to BD shortages [4]. The scarcity of greenhouse gas-emitting fossil fuel reserves is another long-term issue with the current butadiene production method, both in terms of commercial and environmental sustainability. These matters have recently renewed an interest in the century-old heterogeneous catalytic conversion of ethanol to butadiene in which gaseous ethanol is primarily transformed to BD over multifunctional materials.

Scientific development in the production of ethanol from biomass, coupled with state subsidies and mandates, have greatly increased the global output and affordability of bioethanol. Due to its

limited use as a fuel for combustion engines, an excess of bioethanol is expected. For this reason, it is believed that ethanol would make an ideal platform molecule for the synthesis of value-added chemicals, namely butadiene [5]. A recent publication by Bell et al. has detailed the conditions under which the industrial use of butadiene from bioethanol would reduce greenhouse gas emissions; the key is believed to be the use of low-carbon emitting ethanol sources [3]. Another case study by Burla et al. has outlined that the conversion of ethanol and acetaldehyde into butadiene would be profitable under certain given circumstances; butadiene production in the Gulf coast of the USA can be expected to be very profitable as long as ethanol remains below $3.0/gallon [6].

Despite having been successfully implemented in the past, it is recognized that productivity levels of current ethanol-to-butadiene technology are not yet sufficient to insure economic viability [7]. To meet the increasing demand for BD in the face of eventual scarcity, the aim of the ongoing scientific research is to improve the performances of the catalysts being developed.

In the literature, the ethanol-to-butadiene (ETB) reaction is referred to by different names due to the two processes by which it was historically industrialized. The one-step process (or Lebedev process) refers to the direct gas-phase conversion of ethanol to butadiene over active materials. The two-step process (or Ostromislensky process) refers to the conversion to butadiene of an ethanol/acetaldehyde gaseous mixture previously obtained by partial dehydrogenation of ethanol. Because the two processes have been recognized to undergo the same reaction pathway, both can be studied conjointly. BD synthesis through the one-step process usually results in the production of acetaldehyde as a byproduct of the reaction, which has to be recycled in the system in the case of implementation in an industrial process. Thus, even in the one step process it is necessary to test feeds containing acetaldehyde in order to assess the behavior of the catalytic system in acetaldehyde-containing mixtures, however, in lower amounts compared to the two-step process.

Having been discovered more than a century ago, research on the ETB reaction is abundant, but scattered over different time periods. Fortunately, the dispersed literature has been summarized in review articles [4,8–10]; the reader is referred to these publications for details concerning the history of the reaction, its fundamental principles, including mechanistic and thermodynamic considerations, the many catalytic systems studied and the issues regarding the design of new catalysts. Marked by the publication of "Investigation into the conversion of ethanol into 1,3-butadiene" in 2011 by Jones et al. [11] the pace of scientific progress in the field of the ethanol-to-butadiene conversion has accelerated, as illustrated in Figure 1, which indicates the number of publications on the ethanol-to-butadiene reaction in the recent years. The aim of this review is to bridge the gap between the previous reviews dating back to 2014 and the recent advances made in this field. By discussing the latest catalyst designs and characterization techniques, it is hoped that readers wishing to partake in this research can be made fully aware of the newest tools at their disposal to pursue the groundbreaking work accomplished in recent years.
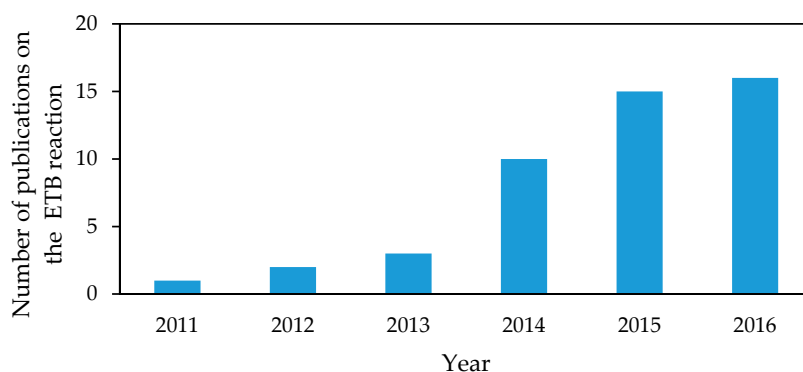


**Figure 1.** Number of publications dedicated to the ethanol-to-butadiene reaction in the recent years. ETB, ethanol-to-butadiene.

*1.2. Reaction Details Reaction of Ethanol to Butadiene*

1.2.1. Generalities Mechanism

Several mechanism explaining the transformation of a gaseous ethanol feed (or an ethanol/acetaldehyde feed) to butadiene have been proposed and debated; the reader is directed to the review article by Sels et al. for the detailed history of this subject [8]. Until recently, the issue was settled by the wide recognition of a mechanism involving the condensation of acetaldehyde as the origin of C4 species. However, based on their observation on purely basic MgO catalysts, Cavani et al. have recently proposed a new and self-consistent mechanism featuring an intermediate carbanion species in the formation of C4 molecules [12–14]. Both will be briefly discussed hereafter. Despite the debate between both mechanisms, the involvement of both ethanol and acetaldehyde in some steps of the reaction is well-established and not controversial [4,8,9]. In general, addition of acetaldehyde (in the two-step process) yields higher butadiene productivity [8]. The reaction can be summarized as a dehydrogenation, condensation, dehydration reaction (Figure 2) for the Lebedev process [14]. Additionally, thermodynamic considerations on the conversion of ethanol to butadiene have also been covered by Sels et al. and Weckhuysen et al. in great detail [8,9].
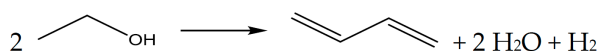


**Figure 2.** Stoichiometry of the ethanol-to-butadiene reaction.

1.2.2. The Kagan Mechanism

The generally recognized route to butadiene formation from ethanol was elaborated over decades by different scientific teams studying the kinetics of the reaction [8]. Because the current form of the mechanism was first proposed by Kagan et al.—subsequently modified by Niiyama et al., Natta et al. and Bhattacharyya et al., it is referred as such in the present paper to distinguish it from the alternative mechanism [4,9]. The complete reaction pathway is believed to proceed as follows (Figure 3): ethanol partially undergoes non-oxidative dehydrogenation, forming acetaldehyde (1); 3-hydroxybutanal (acetaldol) is produced by the adol condensation of two acetaldehyde molecules (2); acetaldol is dehydrated to acetaldehyde (3); crotonaldehyde is subjected to a Meerwein–Ponndorf–Verley–Oppenauer (MPVO) reduction involving ethanol, affording crotyl alcohol and acetaldehyde (4); crotyl alcohol is dehydrated to butadiene (5). The rate-limiting reaction is thought to vary depending on the chemical properties [8]. Over basic catalysts with poor redox properties, ethanol dehydrogenation is generally recognized as the limiting step. In the case of Lewis acids, it is thought to be the MPVO reaction that is the limiting step [8].
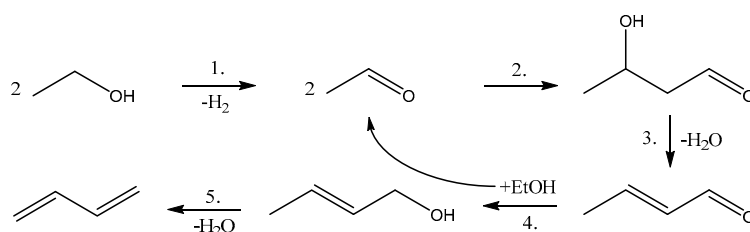


**Figure 3.** Generally accepted reaction pathway for the formation of butadiene from ethanol initially proposed by Kagan et al. [8].

Some issues with this mechanism have been identified by Cavani et al. in their latest book [14]. First, the supposed intermediate acetaldol is seldom detected amongst the products of the reaction, arguably due to its facile dehydration. Second, the engineers at Union Carbide Corporation have

reported that acetaldol was converted back to acetaldehyde when fed together with ethanol into a reactor packed with a 2% Ta/SiO$_2$ catalyst without producing butadiene [15]. This suggests that butadiene is produced through a different route, which does not involve the aforementioned intermediate. Nevertheless, because recent kinetic studies have repeatedly supported the validity of this pathway, it cannot be ruled out [16–19].

### 1.2.3. The Cavani Mechanism

The conversion of ethanol to 1-butanol—through the so-called "Guerbet reaction"—is believed to follow a similar pathway to that of the ETB mechanism indicated above [20–22]. C4 carbonaceous intermediates are thought to be formed by aldol condensation of acetaldehyde, like in the Kagan mechanism, with 1-butanol being formed in the absence of dehydration active sites. However, Meunier et al. have recently argued that aldol condensation was irrelevant [23]. Based on this possibility, Cavani et al. have investigated both reactions over purely basic MgO catalysts at short contact time and proposed new reaction pathways, supported by density functional theory (DFT) calculations, diffuse-reflectance infrared Fourier transform spectroscopy analysis (DRIFTS) and mass spectroscopy (MS) [12,14]. Briefly, the formation of crotonaldehyde was found to be kinetically consecutive to the formation 1-butanol and crotyl alcohol, the precursor to butadiene. Ethylene was also produced in the absence of acid sites, ethanol dehydration thus not being the exclusive pathway to this light olefin. Additionally, the conversion of acetaldol mixed with ethanol did not afford butadiene, but crotonaldehyde and acetaldehyde. A new reaction model was conceived to explain this inconsistency with the Kagan mechanism (Figure 4). According to this model based on observations over MgO, adsorbed ethanol may dissociate into acetaldehyde and hydrogen (1). Ethoxide species adsorbed on specific MgO defects could also undergo proton abstraction to form a carbanionic species stabilized by surface Mg cations (2). This carbanion would act as the main intermediate for the formation of the various products that are generated during an ETB reaction: if attacked by the carbanion, a neighboring adsorbed acetaldehyde molecule would transform into crotyl alcohol (3), which would go on to be dehydrated into BD (4); if attacked by the carbanion, a neighboring adsorbed ethanol molecule would instead form 1-butanol (5), which can be dehydrated into 1-butene (6); in the absence of neighboring molecule, the remaining hydroxy group of the carbanion would dissociate, resulting in ethylene (7).
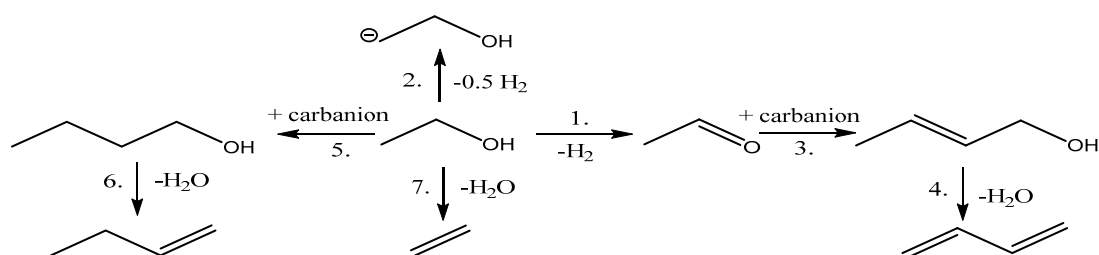


**Figure 4.** Novel reaction pathway for the formation of butadiene from ethanol proposed by Cavani et al. [12–14].

To the best of our knowledge, these very recent results have not been repeated by other teams. On the contrary, subsequent kinetic studies of the ETB reaction and the Guerbet reaction have reconfirmed the original pathways, albeit on other catalysts than MgO [17,18,22].

### 1.2.4. Byproducts

Gaseous ethanol can be easily converted to a wide variety of chemicals with the appropriate catalyst [5]. The product distribution is affected by several factors such as the reaction conditions. A difference in temperature alters the thermodynamics and kinetics of the process, possibly favoring

the formation of byproducts. The same is true for the contact time between the reagents and the catalyst [9,19,24]. Therefore, a careful optimization is required. The nature of the catalysts can also influence the nature and quantity of the byproducts depending on their chemical properties. For instance, silica-supported zirconium oxides were found to produce larger amounts of $C_6+$ hydrocarbon species as side products, presumably due to their trend to catalyze condensation reactions [16]. This issue is complicated by an incomplete understanding of the mechanism. For instance, the formation of ethylene, whether it is directly formed or obtained from diethyl ether cracking, is still a matter of debates and likely depends on the catalyst used [13]. Maximizing the butadiene yield also requires suppressing of the formation of such byproducts [25]. At many steps of the reaction, the intermediate may undergo an alternative pathway, thereby wasting carbon atoms on undesired products. However, the task is complex due to the ambiguity surrounding their formation. Another issue with the formation of several byproducts is the additional cost associated with their separation [25]. Nevertheless, a reaction network of the main byproducts, discussed elsewhere, is summarized in Figure 5 to illustrate the wide variety of species that can be expected and observed [8,16].
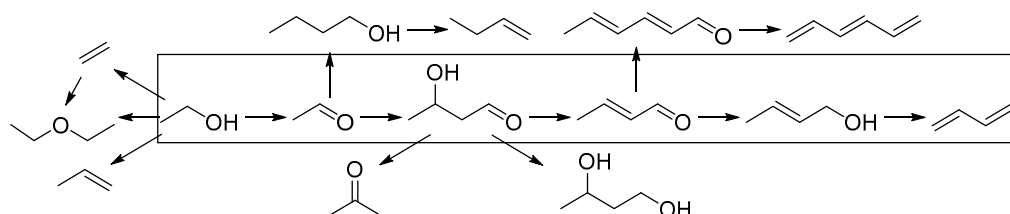


**Figure 5.** Reaction network of the main byproducts [8,16]. The Kagan mechanism intermediates and product are inboxed.

The main byproduct of the ETB reaction is ethylene, which is the result of ethanol dehydration or ether cracking over acid sites. However, dehydration itself cannot be entirely suppressed as it is required for the formation of butadiene after condensation reaction. Other important byproducts include: 1-butanol as a result of the Guerbet reaction, butenes from the dehydration of 1-butanol and propylene, possibly formed by acetone conversion or its own ethanol-to-propylene pathway, as well as $C_5+$ hydrocarbons resulting from the aldol condensation of crotonaldehyde [5,8,16].

### 1.3. Catalyst Design

Due to the variety of reaction steps involved, it is obvious that catalysts for the conversion of ethanol to butadiene must be multifunctional—regardless of the subscribed mechanism. Versatile catalysts have been obtained by mixing different materials to provide the required combined chemical properties. A survey of the literature indicates that active catalytic systems generally have acid, basic or redox properties, or a mixture thereof [8,16]. Redox and basic sites are thought to participate in the dehydrogenation of ethanol to acetaldehyde, while acid and basic active sites have been reported to be active in the reactions of condensation and dehydration [8,9,16]. Because of the complexity of the reaction, a difficult balance between these properties is necessary to achieve for high productivity. The amount of different active sites needs to be in appropriate proportions to avoid promotion of undesired side-reactions, such as dehydration of ethanol. However, definitive identification of the active sites on different catalytic systems remains an open question. As stated by Weckhuysen et al. and summarized by Ivanova et al., a key issue in the design of optimal catalysts is the understanding of the optimal catalytic functions (acid/base/redox), the structure-catalytic relationship and the balance between them [9,16].

Because of the long history of the ETB reaction, several catalytic systems have been proposed. Mixed oxides with either acid, basic and/or redox properties are a significant category of those. Bhattacharyya et al. have thoroughly investigated the potential of binary and ternary metal oxide

systems and discovered that a mixture of amphoteric alumina with basic and redox zinc oxide ($Al_2O_3$-ZnO (60:40)), is the most active catalyst (see Table 1) [26]. Other good catalysts included the mixture of alumina with basic magnesia or alumina with chromium oxide possessing redox properties. Another well investigated catalytic system is MgO-$SiO_2$, which is discussed in more details below.

**Table 1.** Catalytic performances of selected materials of the literature, including the best performing catalysts found in the articles reviewed in this paper.

| ID | Catalyst | $T$ (K) | $WHSV$ ($h^{-1}$) | EtOH/AA | $TOS$ (h) | $X_{EtOH}$ (%) | $Y_{BD}$ (%) | $P_{BD}$ $g_{BD} \cdot g_{cat}^{-1} \cdot h^{-1}$ | Ref. |
|---|---|---|---|---|---|---|---|---|---|
| | | | | Old catalytic systems | | | | | |
| 1 | Wet-kneaded MgO-$SiO_2$ | 623 | 0.15 | - | - | 50 | 42 | 0.06 | [8] |
| 2 | Commercial MgO-$SiO_2$ | 713 | 0.3 | - | - | 70 | 48 | 0.06 | [8] |
| 3 | 2% $Cr_2O_3$-59% MgO-39% $SiO_2$ | 673 | 0.4 | - | - | 68 | 38 | 0.08 | [8] |
| 4 | 3% CuO-56% MgO-42% $SiO_2$ | 673 | 0.7 | - | - | 86 | 44 | 0.22 | [8] |
| 5 | 40% ZnO-60% $Al_2O_3$ | 698 | 1.5 | - | - | 94 | 56 | 0.50 | [26] |
| 6 | 20% MgO-80% $Al_2O_3$ | 698 | 1.5 | - | - | - | 48 | 0.40 | [26] |
| 7 | 40% $Cr_2O_3$-60% $Al_2O_3$ | 698 | 1.5 | - | - | - | 47 | 0.40 | [26] |
| 8 | 9.5% $ZrO_2$-90.5% $SiO_2$ | 698 | 1.0 | - | - | - | 23 | 0.13 | [8] |
| 9 | Ag/$ZrO_2$/$SiO_2$ | 598 | 0.3 | - | - | 34 | 24 | 0.04 | [16] |
| 10 | 40% $ZrO_2$-60% $Fe_2O_3$ | 698 | 1.5 | - | - | - | 40 | 0.34 | [26] |
| | | | | Recent MgO-$SiO_2$ catalysts | | | | | |
| 11 | MgO-$SiO_2$ (WK) | 698 | 1.1 | - | 4 | ~67 [a] | 35 | 0.25 | [27] |
| 12 | MgO-$SiO_2$ (MC) | 673 | 1.0 | - | - | 41.2 | 23.6 [a] | 0.14 | [28] |
| 13 | 3% Au/MgO-$SiO_2$ | 573 | 1.1 | - | 3.3 | 45 | 27 [a] | 0.14 | [3] |
| 14 | 1% Ag/MgO-$SiO_2$ | 753 | 1.2 | - | 3.3 | 84 | 42 | 0.29 | [29] |
| 15 | 1% CuO/MgO-$SiO_2$ | 698 | 1.1 | - | 4 | 74 | 74 [a] | 0.48 [a] | [25] |
| 16 | 1.5% Zr-1% Zn/MgO-$SiO_2$ | 648 | 0.62 | - | 3 | 40 | 30.4 | 0.13 | [30] |
| 17 | 1.2% K/ZrZn/MgO-$SiO_2$ | 648 | 1.24 | - | 3 | 26 | 13.1 | 0.12 | [30] |
| 18 | 2% ZnO/MgO-$SiO_2$ | 648 | 1.0 | - | 3 | 84.6 | 45 | 0.26 [a] | [31] |
| 19 | 1.2% Zn-Talc | 673 | 8.4 [a] | - | 7 | 41.6 | 21.5 | 1.1 [a] | [19] |
| | | | | Recent Zr-containing catalysts | | | | | |
| 20 | 3.5% Ag/Zr/BEA | 593 | 1.2–3.0 | - | 3 | - | - | 0.59 | [32] |
| 21 | 2000 ppm Na/$Zn_1Zr_{10}O_n$ | 623 | 6.2 | - | - | 54.4 | 15.2 [a] | 0.49 | [33] |
| 22 | 2% ZnO-7% $La_2O_3$/$SiO_2$-2% $ZrO_2$ | 648 | 1.0 | - | 3 | 80.0 | 60.0 | 0.71 | [34] |
| 23 | 2% $ZrO_2$/$SiO_2$ [b] | 593 | 1.8 | 3.5 | - | 45.4 | 31.6 | 0.33 [a] | [35] |
| 24 | 4.7% Cu/MCF + 2.7% Zr/MCF [b] | 673 | 3.7 | 0.7–1.6 | 15 | 92 | 64.4 [a] | 1.4 | [36] |
| | | | | Other recent catalytic systems | | | | | |
| 25 | HM-Hf/$SiO_2$ | 633 | 0.64 | - | 10 | 99 | 68.8 | 0.26 | [37] |
| 26 | 3% Ta/BEA [b] | 623 | 0.8 | 3.7 | 4 | 58.9 | 43.1 | 0.20 | [38] |
| 27 | 0.7% Nb/BEA [b] | 623 | 0.8 | 2.7 | 4 | 42.8 | 23.6 | 0.11 | [39] |
| 28 | 1.4% Cr-16% Ba/Al-MCM-41 | 723 | 3.1 | - | 10 | 80 | 22.4 | 0.40 [a] | [40] |

[a] Value estimated according to Equations (1)–(4) based on the data available; [b] used a two-step. WHSV, weighted hourly space velocity in terms of ethanol mass flow; EtOH, ethanol; AA, acetaldehyde; TOS, time on steam.

Apart from mixed oxides, silica-supported Lewis acids for the two-step process have been studied by Corson et al. and Kagan et al. Metal oxides such as zirconium, tantalum, niobium, hafnium, thorium, uranium and titanium oxide were found to be highly active in the conversion of ethanol/acetaldehyde mixtures to butadiene. This was attributed to the ability of these Lewis acids to catalyze aldol condensation, MPVO and dehydration reactions [16].

Another aspect of catalyst design is the recurring use of promoters to tune the properties of the considered catalytic system. Promoters with redox properties (e.g., Ag, Cu, ZnO) have been repeatedly used to enhance the dehydrogenation of ethanol and increase the yield of butadiene in cases where these properties were absent or insufficient in the parent catalyst [4]. For instance, silica-supported tantalum oxide can become active for the Lebedev process with the use of copper to enable to conversion of ethanol to acetaldehyde [41]. The introduction of Lewis acid promoters such as $ZrO_2$ to improve the activity for the MPVO reaction has also been reported over basic catalysts. Alkali metals have been previously used to alter the acid properties by selective poisoning of acid sites or to introduce new basic properties into the catalyst. One notorious case is the introduction of

sodium oxide into MgO-SiO$_2$ by Ohnishi et al., which led to one of the best catalytic performance ever reported [42]. Unfortunately, a lack of experimental details seems to have casted some doubts on the validity of their observations [16].

*1.4. Performances and Reaction Conditions*

Although the economic viability of the ethanol-to-butadiene process is within reach, the current performances do not meet industrial requirements [43–45]. Researchers should therefore strive to design catalysts with improved catalytic performance. As outlined by Jones et al., the most industrially relevant measure of performance is butadiene productivity—meaning the amount of BD produced in relation to the amount of catalyst used over time (e.g., $g_{BD} \cdot g_{cat}^{-1} \cdot h^{-1}$) [7]. Another key factor is the nature and quantity of byproducts, the presence of which leads to decrease of the yield of butadiene and increase the separation costs [25]. In this paper, the catalytic performances will be discussed in terms of BD productivity ($g_{BD} \cdot g_{cat}^{-1} \cdot h^{-1}$), ethanol conversion (%), product selectivity (%) and product yield (%) in terms of molar carbon. The ethanol conversion was calculated according to Equation (1):

$$X\ (\%) = \frac{n_{EtOH}^0 - n_{EtOH}}{n_{EtOH}^0} \times 100\% \tag{1}$$

where $n_{EtOH}^0$ is the number of mole fed into the reactor and $n_{EtOH}$ out of the reactor [34]. Selectivity is calculated by the following Equation (2):

$$S_i(\%) = \frac{n_i \times c_i}{2(n_{EtOH}^0 - n_{EtOH})} \times 100\% \tag{2}$$

where $n_i$ is number of moles of product $i$ and $c_i$ is the number of carbon atoms in product $i$ (e.g., for BD it is equal to 4) [34]. The yield is calculated according to Equation (3):

$$Y_i\ (\%) = S_i \times X \div 100\% \tag{3}$$

Butadiene productivity is estimated using Equation (4):

$$Productivity = Y_{BD} \times WHSV \times 0.587 \div 100\%, \tag{4}$$

where WHSV is the weight hourly space velocity in $g_{EtOH} \cdot g_{cat}^{-1} \cdot h^{-1}$ and 0.587 is the mass ratio between ethanol and butadiene assuming 100% conversion [34].

Apart from its nature, the catalytic performances of a material are largely influenced by the conditions under which they operate. As mentioned above, a proper investigation of the ETB reaction should aim at identifying the best industrial conditions. Obviously, the key conditions are the reaction temperature, pressure and the reactant space velocity. The latter can be expressed in terms of weight hourly space velocity (WHSV), taking in account the mass of catalyst in relation to the mass of gaseous ethanol fed into the reactor. Apart from Bhattacharyya et al., all the publications have dealt with fix-bed reactors [46]. While some researchers have investigated the effect of pressure on the catalytic activity, the reaction is generally conducted at atmospheric pressure; the reviewed literature must be therefore assumed to occur at atmospheric pressure unless otherwise noted [19]. Another parameter that influences the reaction is the catalyst pre-treatment, usually done under inert atmosphere at high temperature to activate the material. Finally, the ratio of ethanol-to-acetaldehyde being fed in a reactor is a crucial factor of the two-step process, as it can influence the BD productivity and product distribution [18,36,41,47,48]. Since several papers have reported different optimal ratios, it is likely that this factor is governed by the nature of the catalytic system and the other reaction conditions.

The catalytic performances found in the literature have been compiled elsewhere [8]. The average results of the best catalysts can be summarized as follows: at temperatures between 573 and 673 K for WHSVs from 0.2 to 1.0 h$^{-1}$, butadiene selectivity is in the range from 40% to 60%, with a butadiene

yield from 30% to 40% [8]. Estimating BD productivity can be difficult due to omission of experimental details, however Jones et al. have suggested a minimum target for butadiene productivity of $0.15\ \mathrm{g_{BD} \cdot g_{cat}^{-1} \cdot h^{-1}}$ before envisioning industrial application [7]. Another crucial factor of the reaction is the time-on-stream (TOS) stability, as costly regeneration is likely to have an impact of the viability of the process. Unfortunately, this parameter is also often ignored, painting an incomplete picture of the catalytic performances, as an undisclosed deactivation may prove to be problematic for industrial applications. When available, this paper will also indicate the TOS at which the activity was recorded. It has been repeatedly demonstrated that the main culprit behind catalytic deactivation was the formation of coke on the catalytic surface [4,36,47,49,50]. Table 1 highlights the performances of notable catalysts for the one-step process reported in the past hundred years to provide references to the readers (catalysts 1 to 10 in Table 1), as well as the catalytic systems reviewed in this work.

## 2. Catalytic Systems

### 2.1. Magnesium-Silica System

#### 2.1.1. Introduction

Magnesia mixed with silica was first reported as an active catalyst for the direct conversion of ethanol to butadiene in 1944 by Szukiewicz [8]. It has been the subject of numerous investigations, making it the most studied catalyst for the ETB reaction. The reader is referred to the review of Sels et al. for a complete survey of the literature prior to 2014 [8]. This section will instead focus on the latest publications on the subject.

As previously stated, the ETB reaction requires multifunctional catalysts active for the various reactions steps believed to be involved: dehydrogenation, dehydration and condensation. The multi-functionality of magnesia-silica catalysts is attributed to the combination of basic and acid properties: the basicity of magnesium oxide is well established, while acidity is attributed to interactions between magnesium oxide and silica [13,29,51]. It has been repeatedly demonstrated that a careful balance of the chemical properties is necessary to maximize butadiene production [8]. In practice, this has often been done by varying the amount of Mg and Si in a material and is expressed by the molar Mg/Si ratio. Although the nature of the active sites is being debated, Kvisle et al. have demonstrated that catalytic activity requires interaction between the magnesia and silica [52]. One issue with the $MgO$-$SiO_2$ system is its susceptibility to deactivate due to coke formation most probably due to the strong basic properties of MgO [53].

Depending on the subscribed mechanism, several active sites and their functionalities have been proposed. Following the Kagan mechanism, basic sites resulting from defects on the MgO phase and Lewis acid-base pair Mg–O are thought to catalyze both the dehydrogenation of ethanol and the aldol condensation between acetaldehyde molecules (Figure 3, steps 1 and 2), incompletely coordinated $Mg^+$ ions, Mg–O–Si Lewis acid and Mg–O acid pairs would then catalyze MPVO reduction (Figure 3, step 4) [54]. The subsequent dehydration to produce butadiene would be catalyzed by acid sites present on the surface of the catalyst (Figure 3, step 5) [29]. In the case of the mechanism proposed by Cavani et al., the MgO surface instead hosts stable carbanions from proton abstraction of ethanol (Figure 4, step 2) [12,13]. Condensation of acetaldehyde with the carbanion leads to the synthesis of crotyl alcohol which dehydrates into butadiene over acid sites (Figure 3, steps 3 and 4). Over bare magnesium-silica, the rate-limiting reaction is thought to be the dehydrogenation of ethanol [24,31,52]. It explains the observed low productivity of butadiene over these catalysts (Table 1).

Recently, Baba et al. have studied the potential of Zn-containing talc as a catalyst [19,55]. Their findings also include observations relevant to the understanding of the magnesia-silica system. To understand the role of magnesia, they have compared the activity of two MgO catalysts prepared by calcination and by hydrothermal treatment. Surprisingly, hydrothermally-treated magnesia was capable of converting ethanol with a conversion of 36.6% and a selectivity of 47.1% towards butadiene at a WHSV of $0.19\ \mathrm{h^{-1}}$ at 673 K. At the same time, calcined MgO did not lead to the formation of BD,

an observation that had previously led several authors to conclude that acidity provided by $SiO_2$ was actually necessary [12,13,27,29,30]. Based on the XPS spectra of $O_{1s}$ for both samples, a correlation was drawn between the formation of butadiene and the presence of a distinct oxygen species in the MgO phase. Baba et al. suggest that this feature plays a key role in the ETB reaction by being an active site for the MPVO reduction of crotonaldehyde to crotyl alcohol and production of acetaldehyde by heterolytic dissociation involving ethanol (Equation (5)).

$$CH_3CH_2OH + \text{O-Mg-O-Mg} \rightarrow \text{O-Mg-H} + \text{H-O-Mg} + CH_3CHO \qquad (5)$$
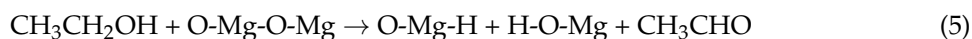
### 2.1.2. Unpromoted MgO-SiO$_2$

Jones et al. have investigated the effect of the Mg-to-Si ratio in MgO-SiO$_2$ catalysts and its effect on catalytic properties [30,44]. MgO-SiO$_2$ was initially prepared by wet-kneading magnesium oxide and silica in water. Subsequently, co-precipitation at 298 K of magnesium nitrate and sodium silicate solutions was employed. For the sake of clarification, wet-kneading is defined as " . . . a process in which two or more solid precursor materials are combined and stirred (mechanically or magnetically) thoroughly in a liquid medium." [27]. The highest butadiene yield has been observed over the catalyst with an optimal Mg/Si ratio above 3. $^{29}$Si cross polarization magic-angle spinning solid-state nuclear magnetic resonance (CP MAS-SSNMR) spectra indicated that silicon atoms in the co-precipitated materials at low Si content consisted largely of Q1 species attributed to single-bridged Mg–O–Si magnesium silicates. XRD also indicated the existence of crystalline MgO in Si-deprived materials, but no correlations with activity have been observed. It was suggested that co-precipitation generated more Mg–O–Si linkages than wet-kneading. Interestingly, an uncalcined Mg(OH)$_2$-SiO$_2$ sample proved to be active in the conversion of ethanol to butadiene. The authors suggest that Mg(OH)$_2$ is also active for the dehydrogenation of ethanol and the aldol condensation, as XRD patterns of the spent catalyst indicate it was not oxidized in situ. The effect of pore size was also studied by using SiO$_2$ with different pore diameters in the preparation of the catalysts. The author reported a drop in ethanol conversion when silica possessing larger pore diameters (250 Å) were used. Preliminary investigations using deuteration indicated that acetaldehyde was converted back to ethanol over MgO-SiO$_2$ catalysts, which was confirmed by the presence of deuterium in the products of ethanol dehydration after having introduced deuterated acetaldehyde into the feed. A kinetic analysis of the reaction was also conducted: results from varying the contact time were in accordance with the Kagan mechanism [24]. Ethanol dehydrogenation was found to be the rate-limiting step at temperatures between 573 and 673 K over MgO-SiO$_2$ (Mg/Si = 1), while aldol condensation would be the slowest step at 723 K.

Weckhuysen et al. have studied the influence of the preparation method on the chemical properties of magnesia silica catalysts [25,27,51]. Wet-kneading, mechanical mixing and co-precipitation were investigated over a MgO-SiO$_2$ catalyst with a Mg/Si ratio of 1. Wet-kneading Mg(OH)$_2$ with spherical silica was found to produce a layered magnesium silicate phase, the presence of which was found to increase butadiene yield. Co-precipitation resulted in a thick amorphous magnesia silicate phase with high ethylene selectivity. Mechanical mixing produced materials with little interaction between the magnesia and silica phases, resulting in poor activity. The acid-base properties of the catalysts were studied using Fourrier transformed infrared (FTIR) spectroscopy coupled with chemisorption of pyridine and deuterated chloroform. It indicated the presence of Brønsted and Lewis acid sites, as well as basic sites of different strengths on the wet-kneaded catalysts. Excessive Lewis acidity and strong basic sites were detected on the co-precipitated materials, which explains the high selectivity to ethylene and the fast deactivation. The use of Hammett indicators further revealed that the catalysts was predominantly basic. TEM images and catalytic testing indicate a closer proximity between magnesia, silica and magnesium, which was correlated with greater catalytic activity. It was argued that a cooperation between acid and basic sites was involved in the ETB reaction. Thus, the best performing catalysts were prepared using nano-sized magnesia particles, which allowed a more intimate mixing between the phases. At 673 K with a WHSV of 1.1 h$^{-1}$ for a TOS of 4 h, butadiene

yield of 35% was achieved, meaning a butadiene productivity of 0.25 $g_{BD} \cdot g_{cat}^{-1} \cdot h^{-1}$ (ID: 11 in Figures 15 and 16). A similarly prepared catalysts was found to be remarkably stable for a period of 24 h. More importantly, the interpretation of solid-state $^1$H-$^{29}$Si CP MAS-SSNMR spectra revealed the existence of distinct magnesium silicates forming at the interface between magnesia and silica–namely anhydrous magnesium silicates, amorphous hydrous magnesium silicates and layered hydrous magnesium silicates. Based on the variation in signal intensity associated to each kind of magnesium silicate and by testing several wet-kneaded samples with different Mg/Si ratios, Weckhuysen et al. were able to directly correlate butadiene yield with the relative amount of layered hydrous magnesium silicates, expressed as the integrated area from the deconvoluted NMR spectra and scaled with number of scans (Figure 6, **left**). Additionally, the relative amount of amorphous hydrous magnesium silicates was directly correlated with ethylene yield (Figure 6, **right**). With these observations, the authors suggested that BD formation could occur on amphoteric layered hydrous magnesium silicates (talc, stevensite, lizardite) close to the MgO phase, while amorphous magnesium silicates contributed to ethanol dehydration, explaining the inferior performances observed with the co-precipitated samples. It was recognized that characterizing the chemical properties and activity of such phases is required to confirm this hypothesis. It should be noted that synthetic talc alone has been demonstrated to be poorly active in the ETB reaction, but was highly active once ethanol dehydrogenation was promoted [19].
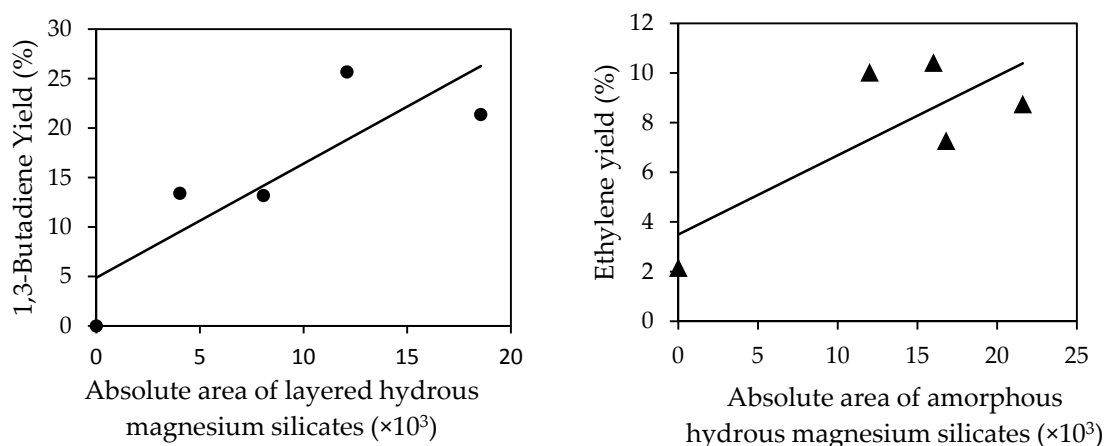


**Figure 6.** Direct correlations between 1,3-butadiene (**left**) and ethylene yield (**right**) and the absolute area detected by $^1$H-$^{29}$Si CP MAS-SSNMR spectroscopy for layered hydrous magnesium silicates (**left**) and amorphous hydrous silicates (**right**), respectively. The areas were determined by scaling the integrals of the corresponding peaks with the number of scans. The data point $x = 0$ is the $MgO_{nano}$ sample. Reprinted with permission from [27]. Copyright 2016, American Chemical Society.

A comparison between mechano-chemically (MC) mixed and wet-kneaded (WK) MgO-SiO$_2$ materials was also conducted by Kyriienko et al. [28]. For the MC mixing process, magnesium oxide and acid-treated commercial silica precursors were ball-milled using inert silicon nitride balls. Powdered XRD indicated the presence of crystalline magnesium silicate forsterite-like phase in the MC mixed sample absent for the wet-kneaded material. Similar phases were also detected for MgO-SiO$_2$ catalysts prepared by co-precipitation and wet-kneading with spherical silica [13,27]. Both materials also displayed intensive signals for crystalline MgO. IR spectra in the OH region revealed that MC mixing consumed Si–OH groups of silica. The authors argue that MC mixing generates localized amorphous magnesium silicates that become crystalline upon heating during the mixing process. Pyridine chemisorption measured by FTIR spectroscopy indicated the presence of weak and strong Lewis acid sites over both samples. However, these sites in MC material weaker. Despite having fewer acid sites and a lower surface area, the MC mixed catalysts turned to be more active and selective towards the formation of butadiene. Further, despite a higher ethanol conversion, the selectivity

towards dehydration products over $MgO$-$SiO_2$ (MC) was half that of $MgO$-$SiO_2$ (WK). The authors attribute this performance to the presence of weak Lewis acid sites capable of participating in the ETB reaction, but less favorable to ethanol dehydration, as well as superior redox properties originating from the crystalline magnesium silicate phase and the proximity between acid and base sites on the surface of the catalyst. At 673 K for a TOS of 8 h and a WHSV of $1\,h^{-1}$, the MC mixed sample displayed a BD yield of 23.7% and a productivity of $0.14\,g_{BD}{\cdot}g_{cat}^{-1}{\cdot}h^{-1}$ (ID: 12 in Figures 15 and 16).

The impact of mixing magnesia with different silica ($SiO_2$, COK-12 & MCM-41) to prepare catalysts for the ETB reaction was evaluated by Sels et al. [29]. $MgO$-$SiO_2$, $MgO$-COK-12 and $MgO$-MCM-41 were prepared by dry milling $Mg(OH)_2$ with the respective silicas based on a Mg/Si ratio of 2. To simulate the effect of impregnation, these materials were treated with water prior to calcination. In the case of $MgO$-$SiO_2$, this approach produced silica particles covered by magnesia flakes. Magnesium silicates were believed to be formed between the two phases. For the materials prepared with mesoporous molecular sieves, their morphology significantly changed by the wetting process. In both cases, a loss of their mesoporous structure and surface area was observed, which was explained by the migration of dissolved magnesium hydroxide into the pores during the wetting process. A collapse of the thin-walled framework was also thought to lead to the formation of amorphous magnesium silicates in the case of MCM-41. The wetting process also altered the surface chemistry of all catalysts. An increase in the amount of both Lewis acid sites and basic sites was observed when compared to the parent materials using FTIR spectroscopy and a thermal conductivity detector (TCD) with chemisorbed $CO_2$ and pyridine. The dispersions of dissolved Mg species could have resulted in additional defects in the magnesia phase, thus generating more basic sites. The dispersion of Mg over silica would also generate Lewis acid sites in the form of isolated Mg(II) cations. The presence of these features was supported by UV–Vis spectroscopy. However, no direct correlation between them and catalytic activity was found as all catalysts displayed very poor ethanol conversion. As discussed below, a silver promoter was used to overcome this problem. Ultimately, the use of COK-12 and MCM-41 produced inferior catalyst as their structure could not survive the preparation method, resulting in restricted access to the potential active sites, as well as reducing the amount of magnesium oxide by forming larger amounts of magnesium silicates.

To measure the validity of their new mechanism, Cavani et al. conducted several experiments using magnesia silica catalysts prepared by the sol-gel technique over a large range of Mg/Si ratios (from 1 to 30) [13]. The Mg/Si ratio was shown to have a significant impact on the structural and chemical properties of each catalysts. At Mg/Si ratios above 9, Si atoms were found to be well dispersed with the magnesia phase, as evidenced by ATR spectra. With Mg/Si ratios between 9 and 3, magnesium silicates were detected by both XRD and attenuated total reflectance, along with crystalline MgO. Only at a ratio of 1 were segregated silica and magnesia phases observed. In situ chemisorption of $CO_2$ measured by DRIFT spectroscopy showed correlation of basicity with Mg content. Conversably, $NH_3$-TCD indicated an increase in acidity associated with larger amounts of silica. These results suggest that the sol-gel technique promotes interaction between $SiO_2$ and $MgO$, but only at low Si content. The variation of the chemical and structural properties had a significant impact on the activity of the catalysts. At high Si content, ethanol conversion into ethylene was the main process (Figure 7). This was attributed to the presence of Mg–O–Si Lewis acid sites generated from the additional Si. The increase in basicity correlated with Mg content and led to an increase of the butadiene yield, despite a drop in ethanol conversion, as the selectivity towards butadiene increased with the Mg/Si ratio (Figure 7). This evidenced the role of the MgO phase in the dehydrogenation of ethanol. However, at a Mg/Si ratio of 30, the overall activity of the material was severely reduced, highlighting the necessity of some acid sites in the process. Interestingly, at low Si content, ethylene selectivity was low, but still detectable as a kinetically secondary product. This phenomenon was explained by the Cavani mechanism, in which the ethoxide carbanion formed on MgO forms ethylene by proton abstraction. An interesting phenomenon was observed when in situ acidity of the catalyst was measured by addition of water in the reactor feed. Pyridine-FTIR revealed an increase in the

number of Brønsted acid sites, which was believed to form during interaction between Lewis acid sites and water. Cavani et al. propose that these sites are responsible for the dehydration of ethanol and crotyl alcohol. This observation also means that ex situ characterization of the catalysts may not give an accurate depiction of the acid-base properties of a catalyst.
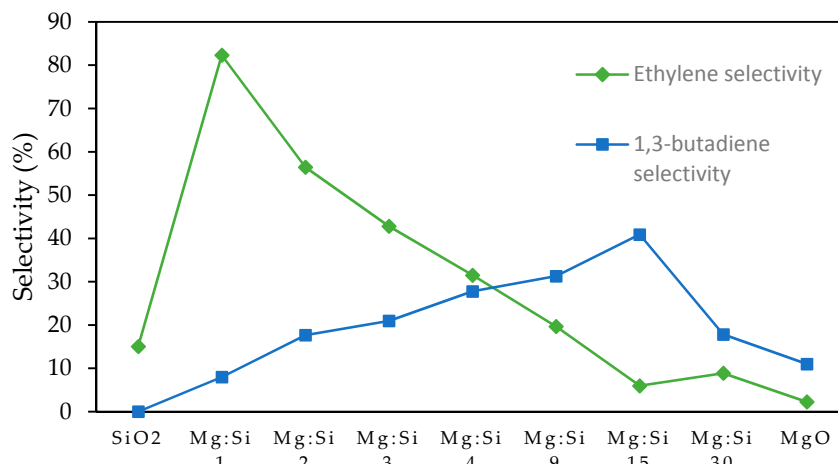


**Figure 7.** Effect of Mg-to-Si ratio on 1,3-butadiene selectivity and ethanol conversion for MgO-SiO$_2$ catalysts prepared by the sol-gel method (*T* = 673 K, contact time = 0.41 s). Reprinted with permission from [13]. Copyright 2016, Royal Society of Chemistry.

### 2.1.3. Metal-Promoted MgO-SiO$_2$

The capacity of noble metals to catalyze the non-oxidative dehydrogenation of ethanol is well established [56,57]. Bell et al. have recently investigated the promotion of ethanol dehydrogenation in the ETB reaction with gold nanoparticles over magnesia-silica catalyst [3]. The catalysts were prepared by impregnation of commercial silica gel with aqueous solutions of magnesium nitrate using IWI method. Materials with Mg/Si ratios from 0.15 to 6 were prepared, dried and calcined at 823 K for 3 h. Au was introduced using a modified deposition-precipitation (DP) method involving the addition of an aqueous solution of HauC$_{14}$ to MgO-SiO$_2$ samples. A pH of 8–10 was reached by adding urea, after which the mixture was dried and reduced under H$_2$. Surprisingly, for materials with Mg/Si ratios above 1, the DP procedure resulted in a disappearance of crystalline MgO and formation of an amorphous magnesium silicate hydrate phase. Transmission electron microscopy (TEM) coupled with energy dispersive spectroscopy (EDS) indicated that Mg and Si were distributed uniformly over the material, suggesting the complete transformation of bulk MgO to the amorphous magnesium silicate hydrate phase. The cause of this phenomenon was subsequently investigated. The authors proposed that silica reacts with water in the presence of HCl produced by hydrolysis of the gold chloride precursor with formation of the magnesium silicate phase. The role of Cl$^-$ was evidenced by the absence of change when the gold precursor was substituted by Au(acetate) and confirmed by the use of HCl$_{aq}$ with magnesium and silica, which also produced the magnesium silicate hydrate phase. The acid-base properties of the catalysts were studied by FTIR spectroscopy. Strong basic sites on the surface of the magnesium silicate were identified using CO$_2$ as probe molecule. Pyridine-FTIR indicated the presence of strong Lewis acid sites, but no Brønsted acid sites were detected. In terms of activity, the materials showed moderately high activity in the Lebedev process. Interestingly, decent ethanol conversion and high butadiene selectivity could be obtained at temperatures as low as 533 and 573 K. Increasing the temperature further only increased ethylene selectivity. High butadiene and acetaldehyde yield, but low selectivity towards dehydration products was reported at 40% ethanol conversion. The optimal catalyst was found to be 3% Au/MgO-SiO$_2$ with a Mg/Si ratio of 1. At 573 K for a WHSV of 1.1 h$^{-1}$, the butadiene yield was 20.5% and butadiene productivity was

$0.14\,\mathrm{g_{BD} \cdot g_{cat}^{-1} \cdot h^{-1}}$ (ID: 13 in Figures 15 and 16). To investigate the active sites of the catalyst, Bells et al. co-fed different reactants and measured their impact on butadiene formation. Unsurprisingly, the addition of acetaldehyde into the feed greatly increased butadiene selectivity. A ten-fold increase in butadiene formation was also observed when crotonaldehyde was co-fed with ethanol, suggesting aldol condensation to be the rate-limiting step. By feeding propionic acid with ethanol to poison the basic sites, it was observed that ethanol dehydrogenation and butadiene formation were suppressed. Although removing the poison from the feed allowed dehydrogenation to recover, butadiene yields remained low. Based on this observation, the authors argue that two different basic sites exist: weak basic sites involved in the dehydrogenation reaction and stronger basic sites active for the aldol condensation—assisted by strong-to-medium Lewis acid sites.

Sels et al. used a silver promoter to enhance performances of their $MgO\text{-}SiO_2$, MgO-COK-12 and MgO-MCM-41 catalysts—poorly active in the dehydrogenation of ethanol [29]. Supported Ag nanoparticles are well-known for their ability to dehydrogenate alcohols in the absence of oxidants [58,59]. Silver particles were introduced into the catalysts by aqueous impregnation with $AgNO_3$ and were subsequently calcined, but were not reduced prior to catalytic testing. Environmental scanning electron microscopy combined with energy diffraction analysis of X-rays clearly indicated that silver nanoparticles were dispersed over the silica phase of the catalysts. The impregnation process also altered the chemical properties of the materials compared to the wetting process. Impregnation reduced the total amount of basic sites. It also increased the relative amount of Lewis acid sites. These alterations were measured by $CO_2$-TCD and pyridine-FTIR. The first observation was attributed to the aggregation of $Mg(NO_3)_2$ species formed by the presence of $NO_3^-$ counter-ions, resulting in large MgO particles possessing fewer basic surface defects. Indeed, the total basicity was shown to decrease with an increase of Ag content. Nevertheless, the overall number of basic sites increased compared to the materials that did not go through a wetting process, meaning Mg(II) dispersion could still occur, albeit at a lesser extent due to $NO_3^-$ counter-ions. The increase in Lewis acid sites is explained by an increase in isolated Mg(II) sites on the silica as a result of the migration of Mg species. The authors also argue that Ag(I) contribute to the Lewis acidity of the material, but due to the likely reduction of silver under the reaction conditions, the quantification of Lewis acid sites could be inaccurate [60]. In terms of activity, a significant improvement was observed on all samples, but was more pronounced with $MgO\text{-}SiO_2$ and MgO-COK-12 than on MgO-MCM-41. The latter phenomenon is believed to occur as a result of the smaller pores of the molecular sieve, more susceptible to the negative effects of impregnation discussed above (pore blockage and structure collapse), ultimately hindering the access to silver active sites. The promotion of ethanol dehydrogenation shifted the limiting reaction to aldol condensation, as evidenced by the accumulation of acetaldehyde. However, excessive amount of silver lead to decrease in activity, likely due to the formation of large Ag particles [58]. Based on this observations, Sels et al. recommend an optimal amount of silver as 1–2 wt %. Ultimately, the most active catalyst was reported to be 1% $Ag/MgO\text{-}SiO_2$ with a BD yield of 42% and a productivity of $0.29\,\mathrm{g_{BD} \cdot g_{cat}^{-1} \cdot h^{-1}}$ at 753 K for a WHSV of $1.2\,\mathrm{h^{-1}}$ after 200 min on stream (ID: 14 in Figures 15 and 16).

Weckhuysen et al. have investigated the addition of CuO to magnesia-silica materials [25,50,51]. The best catalyst was found to be 1 wt % $CuO/MgO\text{-}SiO_2$ prepared by impregnating the wet-kneaded magnesia-silica catalysts discussed above with copper salt using the IWI method. XRD indicated that copper was isolated over the catalyst surface. At 673 K with a WHSV of $1.1\,\mathrm{h^{-1}}$ for a TOS of 4 h this catalyst showed a total butadiene yield of 74% and a butadiene productivity of $0.48\,\mathrm{g_{BD} \cdot g_{cat}^{-1} \cdot h^{-1}}$, a great improvement from the unpromoted material, which showed a total butadiene yield of 32% under the same conditions (ID: 15 in Figures 15 and 16). This increase in activity is primarily attributed to the redox properties of copper, which promotes the dehydrogenation of ethanol to acetaldehyde. A secondary contribution could come from the selective poisoning of the stronger acid sites by CuO. Interestingly, the promoter effect of CuO was more pronounced when it in contact with the magnesia phase—either by post-synthesis IWI or by co-precipitating CuO with MgO before wet-kneading in $SiO_2$. This improvement prompted an intensive study on the relation between the

two metal oxides using X-ray absorption near edge structure (XANES) and extended X-ray absorption fine structure (EXAFS). Ex situ analysis showed Cu(II) to be the predominant specie, existing as a distorted octahedral in a $Cu_xMg_{1-x}O$ solid solution. However, under reductive operando conditions at 698 K, a quasi-steady-state was quickly obtained with the introduction of ethanol during which approximately 60% of the total copper was reduced to its metallic state, 20% to its $Cu^{1+}$ state and a final 20% remaining unchanged. The authors conclude that the metallic species was responsible for the dehydrogenation of ethanol, but that the remaining CuO could still contribute to the performances by poisoning the stronger acid sites. Contrarily to the bare catalyst that did not deactivate, a slight but constant deactivation was also observed with the copper-containing catalyst over a period of 24 h. Because no increase in the amount of Cu–Cu bonds was detected by X-ray adsorption spectroscopy (XAS), it was instead attributed to coke formation, and not metal aggregation.

### 2.1.4. Lewis Acid Promoted MgO-SiO$_2$

Jones et al. have investigated the use of mixed zinc and zirconium oxides as promoters for the MgO-SiO$_2$ catalysts mentioned above which were prepared by wet-kneading and co-precipitation at a variety of Mg-to-Si ratios [30,44]. 1.5 wt % Zr(IV) and 0.5 wt % Zn(II) were introduced by simultaneous aqueous impregnation with the appropriate salts, followed by calcination. Contrarily to other reports, Jones et al. tested the effect of not calcinating their MgO-SiO$_2$ catalysts before impregnation, a procedure which lead to a comparatively greater surface area when using the co-precipitation method. Compared to the bare catalysts prepared by wet-kneading, the addition of ZnO and ZrO$_2$ greatly improved the selectivity towards butadiene with a slight increase in ethanol conversion. Over MgO-SiO$_2$ catalysts, the rate-limiting reaction is believed to be ethanol dehydrogenation. When doped with zinc oxide, a change of the rate-limiting step to subsequent reactions can be expected to occurs, most notably to aldol condensation (according to the Kagan mechanism) due to the often observed accumulation of acetaldehyde and to kinetic studies [3,24,29]. In that case, the promotion of such a reaction would become beneficial. It was suggested that both zinc and zirconium oxides possessed the Lewis acidity believed to be capable of catalyzing the aldol condensation [11]. The increased performances of doped MgO-SiO$_2$ are suggested to be result of improved redox properties by ZnO and a promotion of aldol condensation by the zinc and zirconium oxide couple. Contrarily to their observations with the bare magnesia-silica catalysts where higher Mg content improved the activity for both the dehydrogenation and condensation reactions, Jones et al. found that the optimal Mg-to-Si ratio for Lewis promoted catalysts was of 1. ZrO$_2$ and ZnO are likely to disperse more readily over Mg–O–Si linkages to form smaller, more active particles. Therefore, MgO-SiO$_2$ catalysts with greater Si content would benefit more from the promoter effect. According to $^{29}$Si MAS NMR results, co-precipitation was found to be more efficient at generating these linkages at a Mg/Si ratio of 1 when compared to wet-kneading. Furthermore, a drop in activity was observed at high Si content, suggesting a necessary contribution of magnesia to the process. A combination of the promoter effects provided by ZrO$_2$/ZnO and the increased dispersion resulting from the additional Mg–O–Si linkages is thought to be the origin of the superior performances of 1.5% Zr-0.5% Zn/MgO-SiO$_2$. At 648 K with a WHSV of 0.62 h$^{-1}$ for a TOS of 3 h, the total butadiene yield was of 40% for a productivity of 0.13 $g_{BD} \cdot g_{cat}^{-1} \cdot h^{-1}$ (ID: 16 in Figures 15 and 16). The doped catalysts were further modified by introducing alkali metal (Na, K and Li) through impregnation, resulting in a suppression of ethanol dehydration, as well as an increase in butadiene and acetaldehyde selectivity, albeit at the expense of ethanol conversion (Figure 8). CHCl$_3$-FTIR indicated that alkali modification did not greatly alter the basicity of the catalysts, the changes in catalytic activity were therefore attributed to deactivation of stronger acid sites, as measured by NH$_3$-FTIR. Although the best alkali doped catalyst did not result in high butadiene yield, it nevertheless offers the possibility of recycling the large amounts of acetaldehyde produced, while benefiting from the reduced ethylene production. In that sense, the best performing catalyst was 1.2% K/1.5% Zr-0.5% Zn/MgO-SiO$_2$ with a combined butadiene-acetaldehyde selectivity of 72% (ID: 17 in Figures 15 and 16).
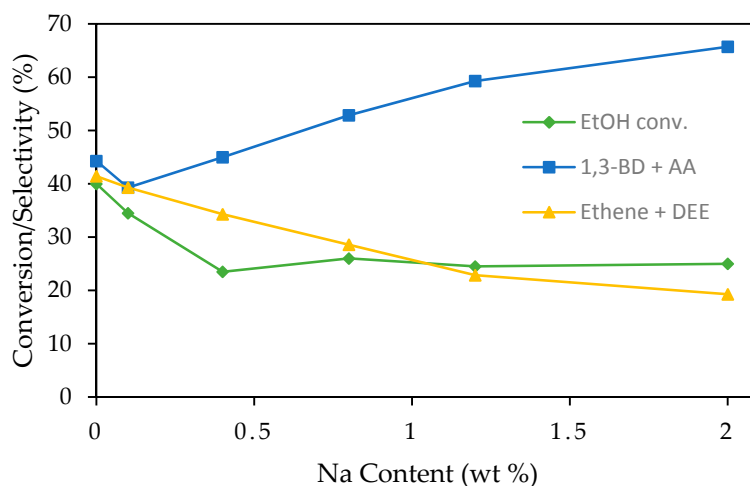
**Figure 8.** Effect of catalyst Na content on ethanol conversion and selectivity towards the main categories of products (*T* = 648 K, weight hourly space velocity of ethanol (*WHSV*) = 0.62 h$^{-1}$, time on stream (*TOS*) = 3 h). Reprinted with permission from [30]. Copyright 2016, John Wiley and Sons.

Kyriienko, Larina et al. have also investigated the use of zinc and zirconium as promoters for MgO-SiO$_2$ catalysts [31,61]. The effect of ZnO alone on the catalytic system was first studied [31]. MgO and silica gel mixed at different ratios were impregnated by zinc acetate solutions, dried and calcined for three hours. MgO and SiO$_2$ were also impregnated in the same way for comparison. Catalytic tests at temperatures ranging between 623 and 698 K and with WHSVs between 0.45 and 1.0 h$^{-1}$, along with characterization of the samples were conducted. Pyridine-FTIR revealed the existence of two types of Lewis acid sites on ZnO/MgO-SiO$_2$: one exclusive to MgO-SiO$_2$ and another resulting from the interaction between ZnO and SiO$_2$. The latter coincided with the pyridine chemisorption IR spectra over ZnO/SiO$_2$ and was found to gain in signal strength with ZnO/MgO-SiO$_2$ possessing larger amounts of Si. The dispersion of all elements of the catalysts was evidenced by XRD and XPS-EDS. In terms of catalytic activity, zinc oxide was found to improve the formation of butadiene of MgO-SiO$_2$ catalytic system. However, at higher Mg-content, ethanol conversion dropped from 56% to 32% and down to 10% over ZnO/MgO. Higher Si-content led to increase of ethanol dehydration products, a trend which continued over to ZnO/SiO$_2$ and attributable to the formation of new acid sites by zinc oxide on silica. As a result, the optimal Mg/Si ratio for the production of butadiene was found to be 1. At 648 K with a WHSV of 1.0 h$^{-1}$ and a TOS of 3 h, 2% ZnO/MgO-SiO$_2$ had a reported yield of 45% and a productivity of 0.26 g$_{BD}$·g$_{cat}^{-1}$·h$^{-1}$ (ID: 18 in Figures 15 and 16). The improved performance of the material was attributed to the promotion of ethanol dehydrogenation by ZnO dispersed on the silica. The presence of equal amounts of magnesia and silica was necessary to properly catalyze the subsequent reaction steps. The addition of zirconium to the above system was evaluated in a following study [61]. Before impregnation with a zinc acetate solution, zirconium oxynitrate hydrate was mixed with pre-calcined MgO, SiO$_2$ and both, followed by the addition of water. In terms of activity, the addition of ZrO$_2$ to the mixture of SiO$_2$ and MgO doubled the conversion of ethanol without significantly altering the selectivity towards butadiene, ethylene or acetaldehyde. However, an increase of C$_5$+ side products was observed, attributed to the condensation of crotonaldehyde promoter by ZrO$_2$ and noted with similar catalysts [16]. The mixture of ZrO$_2$ with MgO-SiO$_2$ and SiO$_2$ formed new Lewis acid sites not observed on ZrO$_2$/MgO or bare magnesia-silica. The involvement of these additional sites is not evidenced, however the authors suggest they may improve acetaldehyde condensation due to a synergic effect with magnesia and silica. Surprisingly, the addition of ZnO to the ZrO$_2$-MgO-SiO$_2$ system did not significantly improve its performances, a phenomenon explained by a suppression of the acid sites believed participate in the reaction. This also explains the reduction of dehydration products. Surprisingly, the addition of ZnO

lead to significant improvements to the performances of $ZrO_2$-$SiO_2$, greatly increasing both ethanol conversion and selectivity towards butadiene, resulting in a better catalyst than $ZnO/ZrO_2$-$MgO$-$SiO_2$. At 648 K with a WHSV of 1.0 h$^{-1}$ and a TOS of 3 h, 4% $ZnO$/6% $ZrO_2$-$SiO_2$ showed a butadiene yield of ~50%, resulting in a butadiene productivity of ~0.29 $g_{BD} \cdot g_{cat}^{-1} \cdot h^{-1}$. Silica-supported zirconium oxide with ethanol dehydrogenation promoters have been reported as highly active and are discussed below [11,16]. The discrepancy with the observations of Jones et al. can be explained by differences in the preparation methods.

### 2.1.5. Promoted Magnesium Silicate Minerals

Magnesium silicate clay minerals have also been used as catalysts for the conversion of ethanol to butadiene [8]. In particular, sepiolite was previously the subject of investigations, including modifications with Ag, Cu, Ni, Co, V and Zn [8,62–64]. Recently, Baba et al. have studied the potential of Zn-containing talc as a catalyst [19,55]. A thorough optimization of the experimental conditions was conducted. Ethanol conversion was found to greatly influence the product distribution: maximum butadiene selectivity and productivity was observed at an ethanol conversion of approximately 50%. In practice, ethanol conversion was purposefully maintained at 40%. Concerning the effect of catalyst preheating, it was found that heating the catalyst at 673 K for 8 h was optimal; higher temperatures and shorter periods were detrimental to butadiene production. The rate of butadiene formation was found to be proportional to ethanol pressure after decreasing it to 20 kPa with the product distribution only slightly affected—indicating the first-order nature of the reaction. The best performing catalyst was reported to be 1.2% Zn-talc, displaying a butadiene yield of 21.5% and a butadiene productivity of 1.01 $g_{BD} \cdot g_{cat}^{-1} \cdot h^{-1}$ at a WHSV of 8.39 h$^{-1}$ and a temperature of 673 K (ID: 19 in Figures 15 and 16). To the best of our knowledge, this makes Zn-containing talc the most productive catalyst for the one-step process. The role of zinc in this system was also thoroughly investigated by means of characterization, reactivity tests and DFT studies. Modified talc was prepared by hydrothermally synthesizing talc in an autoclave with the addition of zinc precursors. The presence of zinc was found to significantly suppress the dehydration of ethanol. Over pure talc, the combination of ethylene and diethylether accounted for 77.5% of carboneous products; the addition of zinc lowered this value to a minimum of 6.4% at the reaction conditions described above. In return, selectivity towards acetaldehyde and butadiene greatly increased up until Zn concentration of approximately 2 wt %. This improvement observed was solely attributed to the promotion of ethanol dehydrogenation, as the reaction of an acetaldehyde feed revealed that the presence of zinc actually suppresses crotonaldehyde formation, which is the secondary product of aldol condensation. The effect of zinc incorporation on the chemical properties of talc was evaluated to explain the promoter effect. The substitution of magnesium by zinc in the octahedral sites of the talc lattice was evidenced by XRD. The binding energies of $Mg_{2p}$, $Si_{2p}$ and $O_{1p}$ were measured using XPS. Although Si and Mg were unaffected, the binding energy $O_{1s}$ was reduced with increased zinc concentration isn talc. It was assumed that the introduction of Zn resulted in a decrease in the basicity of talc, correlating with the reduction of croton aldehyde formation observed as it is believed to occur on basic sites. The origin of the dehydrogenative properties of Zn-talc was investigated using DFT studies to estimate the chemical hardness of the material, according to the theory elaborated by Pearson and Parr [65]. In short, zinc introduction is believed to soften the chemical hardness of talc, turning into a soft Lewis acid with an increased electronic polarizability of its O atoms. Doing so would enhance dehydrogenation of ethanol by promoting hydride abstraction of the –$CH_2$–O– group in surface ethoxide formed by ethanol chemisorption due to its soft Lewis basic nature. According to the theory of hard and soft acids and bases, the highly polarizable and low positively charged soft Lewis acids reacts more readily with low electronegative and high polarizable soft bases [66]. In this case, DFT computations were employed to estimate the alteration of chemical hardness based on bandgap between the highest occupied crystal orbital (HOCO) and lowest occupied crystal orbital (LUCO) energy levels of the crystal before and after the incorporation of zinc. The authors suggest that the concept of chemical hardness coupled with

computational calculations could be a useful tool to predict the promoting effect of dopants introduced in catalytic systems for the ETB reaction.

*2.2. Zirconium Catalytic System*

2.2.1. Introduction

Lewis acid catalysts consisting of silica-supported zirconium, tantalum and niobium oxide were investigated several decades ago for the Ostromislensky process by Toussaint et al. [67]. After a screening study, Jones et al. concluded that zinc and zirconium oxide on silica were active in the Lebedev process due to a combination of Lewis acidity and the capacity of ZnO to catalyze the dehydrogenation of ethanol [11]. Recently, Ivanova et al. outlined a novel approach to the design of catalysts for the Lebedev process. By combining metal oxides active in the aldol condensation and the MPVO reduction ($ZrO_2$, MgO, $Al_2O_3$, $Nb_2O_5$, $TiO_2$) with metal promoters capable converting ethanol to acetaldehyde (Ag, Cu, Ni) over silica, the team was able to produce highly active materials for the one-step process [16]. Early investigations having identified silver/zirconium system as the most active for the production of butadiene, it was thoroughly investigated. Such investigations include: the aldol condensation of acetaldehyde over silica-supported zirconium oxide, the dehydrogenation of ethanol over silica-supported silver and the MPVO reduction of crotonaldehyde over Zr-containing catalyst—all reactions believed to occur in the Kagan reaction pathway [54,59,68].

2.2.2. Catalysts for the One-Step Process

Ivanova et al. have investigated the use of ordered microporous zeolite beta polymorph A (BEA) and mesoporous MCM-41 as alternatives to silica to support their Ag and Zr(IV) catalytic system [69]. At equal amounts of silver and zirconium, the BEA-supported catalyst was found to slightly more active than the MCM-41 catalyst and significantly better than its silica-supported equivalent. The higher activity observed with molecular sieves was explained by the greater concentration of isolated Zr(IV) sites that could be obtained by directly incorporation during the synthesis procedure and evidenced by XPS and $^{29}$Si MAS NMR, as opposed to the impregnation of silica, where zirconium is supposed to be in the form of $ZrO_2$. The butadiene yield also correlated with the amount of Lewis acid sites, identified by FTIR using deuterated acetonitrile ($CDCN_3$) and attributed to the isolated Zr(IV) sites. In all the samples, the dry impregnation with silver lead to the formation of 2–5 nm particles, the optimal particle size for the dehydrogenation of ethanol when supported over silica [58]. Although Ag/Zr/BEA and Ag/Zr/MCM-41 displayed similar activity, the latter generated more dehydration products due to the greater amount of surface silanol groups acting as Brønsted acid sites. The nature of Zr/BEA active sites was further investigated in subsequent studies [49,70]. Ivanova et al. argued that the configuration of Zr(IV) within the zeolite framework influenced the activity of the Lewis acid sites—a phenomenon comparable to the well-documented cases of Ti/BEA and Sn/BEA in which distinguishable "open" and "closed" Lewis acid sites have been demonstrated to exist [71–75]. The term open site refer to partially hydrolyzed metal ion sites linked by three M–O–Si bonds to the zeolite framework with one M–OH linkage (Figure 9) compared to closed sites fully coordinated in the zeolite framework by four M–O–Si bonds (Figure 9).
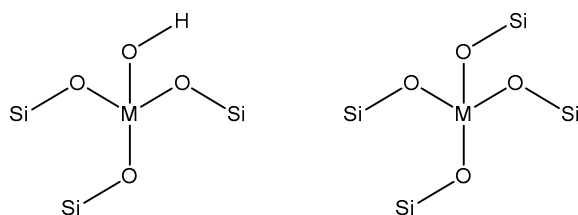


**Figure 9.** Distinct open (**left**) and closed (**right**) metal ion sites in M/BEA (M = Zr, Sn, Ti) [49,70–75].

The presence and role of open Zr sites was subsequently demonstrated on Zr/BEA prepared by hydrothermal synthesis according to the literature with ZrOCl$_2$ as a precursor [76]. Due to the subtle difference between open and closed sites, clearly identifying the nature of the Lewis acid site required the chemisorption of multiple molecular probes measured by FTIR spectroscopy. The presence of weak Brønsted acid sites could only be demonstrated by ditertbutylpyridine (DTBPy)-FTIR, a sensitive probe when compared to pyridine, which failed to show any Brønsted acidity at all. As bulk ZrO$_2$ shared similar bands, its signal was tentatively assigned to interaction with Zr–OH bonds. Contrarily to Ti/BEA, distinguishing between the open and closed Lewis acid could not be done using deuterated acetonitrile as a probe, as it only displayed a single signal for Zr/BEA Lewis acid sites. Carbon monoxide (CO) chemisorption at low temperature was used to address this issue. The progressive adsorption of CO unto the catalyst surface monitored by FTIR spectroscopy revealed the presence of two different Lewis acid sites—one strong, one weak—as well as the presence of an OH group, also attributed to a Zr–OH group and thought to belong to the open Lewis acid site. To demonstrate this, CDCl$_3$ was preadsorbed on Zr/BEA before adding CO at low temperature; this resulted in a significant suppression of the CO signals for Zr–OH and the strong Lewis acid site. It was therefore concluded that both signals belong to the same species: the open Lewis acid sites, and that CDCl$_3$ exclusively adsorbed unto it, sterically hindering the access to CO. Only the latter could properly distinguish between both sites. With a method to detect Zr open and closed sites, Ivanova et al. were able to compare their relative amounts with the formation of butadiene from ethanol obtained during catalytic testing [32,49]. A direct correlation between the relative number of open Lewis acid sites and the initial rate of butadiene production was observed (Figure 10). On the contrary, the relative amount of closed sites did not correlated with the conversion of ethanol, suggesting that they are either inactive or less active in the ETB reaction [49].
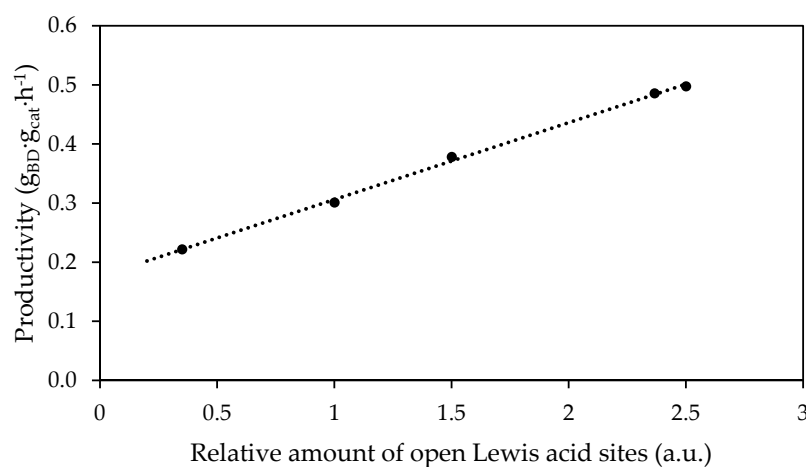


**Figure 10.** Correlation between the relative amount of open Lewis acid Zr sites with the rate of BD formation. Adapted from [32]. Copyright 2016, WILEY-VCH Verlag GmbH & Co. KGaA.

Having identified the nature of the active sites, Ivanova et al. focused on designing more active catalysts by maximizing the amount of open sites [32]. To this end, a new approach to the preparation of Ag/Zr/BEA was developed. By the post-synthetic treatment of dealuminated BEA zeolite with a DMSO solution of ZrOCl$_2$ under reflux conditions, catalysts containing only open Zr Lewis acid sites were obtained, as evidenced by the FTIR spectroscopy method described above. It was discovered that the grafting of zirconium ions over terminal silanol groups, which can be found on the surface of zeolites, led to the formation of the desired open Zr sites and that this particular post-synthetic treatment highly favoured the interaction between the dissolved precursor and such groups. Surprisingly, Zr was not grafted onto the silanol groups formed during the dealumination with nitric acid, the so-called "silanol nests", meaning these had little impact on the incorporation of

zirconium. These phenomena was evidenced FTIR spectroscopy in the O–H region, demonstrating a consumption of terminal silanol groups by the post-synthesis procedure, but not of silanol nests. Steric hindrance, diffusion limitations or energetic limitations were suggested as the cause of this preferential grafting. The relative amount of open Lewis sites was measured by CO-FTIR and correlated with the crystal size of zeolite—smaller crystals possess additional terminal silanol groups, resulting in greater amounts of open sites. In turn, ~1% Ag/Zr/BEA catalyst was significantly more active than those prepared by the traditional hydrothermal route. The most active amongst them was ~3.5% Ag/Zr/BEA with Si/Zr ratio of 75; it achieved a selectivity towards butadiene near 60% and a productivity of $0.58 \, \mathrm{g_{BD} \cdot g_{cat}^{-1} \cdot h^{-1}}$ (ID: 20 in Figures 15 and 16). This places the catalytic system designed by Ivanova et al. amongst the most productive currently recorded. Although the precise WHSV is not disclosed, it is indicated to be between 1.2 and 3.0 $\mathrm{h^{-1}}$.

Wang et al. have studied the conversion of ethanol to butadiene over a zinc-zirconium mixed oxide catalytic system, adding sodium to alter its surface acidity and further studied the relation between the material's chemical properties and catalytic activity [77]. $Zn_xZr_yO_z$ was synthesized using commercial carbon as a hard template for impregnation with different amounts of dissolved zinc and zirconium precursors. The template was removed by calcination at 823 K for 20 h, affording a zirconia material over which zinc oxide is highly dispersed, according to XRD patterns. As per a previous publication by the same research team, such a material would also possess large mesopores [77]. As demonstrated with $NH_3$-TPD and pyridine-FTIR, varying the Zr/Zn ratio from 2 to 30 had a significant impact on the surface acidity of the catalytic system. On all samples, weak, medium and strong Brønsted and Lewis acid sites were detected. Decreasing the Zr/Zn ratio from 30 to 10 weakened the strength of the acidity, generating greater amounts of weak and medium sites at the expense of strong sites. This alteration mostly affect the Lewis acidity of the sample. Below a ratio of 10, the Brønsted acidity of the material was suppressed and the number of sites of all strength dropped. It was suggested that zinc oxide first passivates strong Lewis acids, then targets medium Brønsted acid sites. New Lewis acid sites could also be generated with sufficient interaction at oxygen vacancies of mixed zinc-zirconium oxide phase. These changes in surface chemistry were reflected in the catalytic activity of the samples: the loss of Brønsted and strong Lewis acid sites due to the suppression by zinc oxide was associated with a reduction in the quantity of dehydration products. It also led to the accumulation of acetaldehyde, which evidenced that the rate-limiting reaction step shifted from ethanol dehydration to aldol condensation due to the redox properties introduced by zinc oxide. However, at the highest Zn content, the overall ethanol conversion and butadiene selectivity dropped, suggesting that Brønsted acid sites might be necessary for the reaction. A catalyst without Brønsted acidity was prepared by incipient wetness impregnation to verify this possibility; it mostly produced acetaldehyde and crotonaldehyde, but little butadiene or ethylene. Although the authors argue that this observation demonstrates the role of Brønsted acid sites in the reaction, there is a possibility that different structural properties, namely the great surface area of the templated catalyst, might have played a role. Because the loss of Brønsted acid sites also suppressed ethylene formation, the alteration of surface chemistry with Na was attempted over the mixed oxide with a Zr/Zn ratio of 10. Evidenced by FTIR spectroscopy with molecular probes, the addition of sodium shifted the strength of acid sites from strong and medium to medium and weak. It also reduced the overall amount of sites with increased Na amount, while retaining both types of acidity. These changes greatly reduced ethanol dehydration, simultaneously increasing acetaldehyde and butadiene formation. The suppression of ethylene formation was attributed to the passivation of strong acid sites by Na-doping, while preserving sufficient medium-strength acid sites of both types to catalyze the desired reaction. Figure 11 illustrates the effect of Na doping at increasing amounts on the catalytic performance of the catalyst. For the catalytic testing of 2000 ppm $Zn_1Zr_{10}O_n$ at 623 K for a WHSV of 0.2 $\mathrm{h^{-1}}$, ethanol conversion was 97% with a high selectivity towards butadiene of 47% and ethylene selectivity of 15.9%. In addition, the catalyst remained reasonably active at a high WHSV of 6.2 $\mathrm{h^{-1}}$ producing butadiene at a rate of 0.49 $\mathrm{g_{BD} \cdot g_{cat}^{-1} \cdot h^{-1}}$ with an ethanol conversion of 54.4% and a BD selectivity of 28%. In terms

of stability, a 20% drop in ethanol conversion was observed over a period of 60 h, along with a slow decay of butadiene selectivity to the benefit of acetaldehyde formation. The deactivation was reversed with calcination under air, suggesting coke formation as its origin.
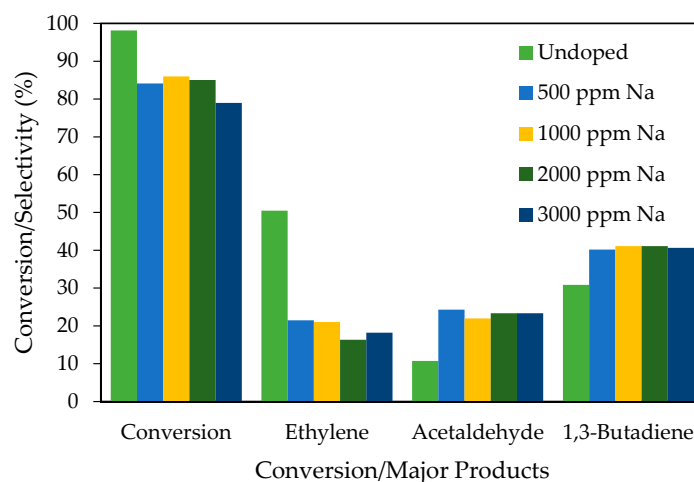


**Figure 11.** Effect of Na-doping on the conversion and selectivity towards major products on $Zn_1Zr_{10}O_n$ catalyst ($T$ = 623 K, *WHSV* = 0.2 h$^{-1}$). Reprinted with permission from [33]. Copyright 2014, Elsevier.

Kyriienko et al. have investigated the use of silica-supported lanthanum oxide as an active component of mixed oxide catalyst including zing and zirconium for the one-step conversion of butadiene [34]. Lanthanum was previously reported active for several of the reaction taking part in the Kagan mechanism, namely ethanol dehydrogenation, aldol condensation and the MPVO reduction [78–80]. Silica was prepared from treated commercial silica gel and was impregnated with lanthanum nitrate hexahydrate and/or zinc acetate solution by the incipient wetness impregnation (IWI) method. Zirconium was added to the mixture by wet-kneading zirconium oxynitrate with silica. The samples were subjected to catalyst activity testing at 648 K at a WHSV of 1.0 h$^{-1}$. At TOS of 3 h, 7% $La_2O_3/SiO_2$ was shown to catalyze the formation of butadiene with a selectivity of 23%. However, ethanol conversion remained low and dehydration products were the main products. The addition of zinc to this system increased ethanol dehydrogenation—evidenced by increased production of acetaldehyde and suppression of dehydration. When $ZnO$-$La_2O_3/SiO_2$ was mixed with zirconium, a significant increase in butadiene formation was observed. 2% $ZnO$-7% $La_2O_3/SiO_2$-2% $ZrO_2$ greatly increased ethanol conversion to 80% while keeping the selectivity towards dehydration products below 14%. Butadiene selectivity increased to 65.7% while acetaldehyde selectivity fell sharply, a sign of increased activity in the reaction believed to be aldol condensation. At 648 K for a WHSV of 2 h$^{-1}$ and a TOS of 3 h, this material showed a butadiene yield of 60% and a productivity of 0.71 $g_{BD} \cdot g_{cat}^{-1} \cdot h^{-1}$, making it one of the best performing catalyst for the one-step process (ID: 20 in Figures 15 and 16). Additionally, the catalytic activity was maintained for 10 h. Acid and base surface properties of this system were characterized by pyridine-FTIR and pyrrol-FTIR. Signals believed to belong to basic sites were attributed to the addition of lanthanum oxide to silica while Lewis acid sites were assigned to the presence of zirconium, and to a lesser extent to lanthanum and zinc oxides interacting with the silica phase. Based on these observations, the authors explain that the high activity as a synergic effect between each component of the system: lanthanum oxide and zirconium oxide are thought to provide basic sites and Lewis acid sites respectively, while zinc oxide would promote the dehydrogenation of ethanol; the combination of acid, base and redox properties meet the criteria to catalyze the ETB reaction based on the Kagan mechanism. This conclusion is further supported by the high selectivity towards butadiene but poor ethanol conversion observed with 7% $La_2O_3/SiO_2$-2% $ZrO_2$, in which case the rate-limiting reaction should be the ethanol dehydrogenation.

### 2.2.3. Catalysts for the Two-Step Process

Han et al. have examined $ZrO_2/SiO_2$ catalysts for the Ostromislensky process. Using a sol-gel method with nitric acid to induce hydrolysis and gelification of tetraethyl orthosilicate (TEOS), different catalysts were prepared with $ZrO_2$ content going as high as 8.4 wt %. The gels were dried and calcined at 823 K for 6 h, affording mesoporous materials with large surface area that decreased with the increase in $ZrO_2$ content. Because no $ZrO_2$ phase was observed by XRD, it was assumed to be highly dispersed despite the high zirconium loading and further evidenced by TEM, which also revealed the catalyst possessed a leaf-like morphology. Brønsted and Lewis acid sites were detected by pyridine-FTIR spectroscopy, but only Lewis acid sites were shown to increase with higher zirconium content. The catalytic activity was measured according to three controlled parameters: temperature, WHSV and ethanol-to-acetaldehyde ratio. While increasing the temperature from 593 to 683 K promoted ethanol conversion, it also promoted butenes selectivity at the expense of butadiene formation. WHSV did not affect butadiene selectivity, but reduced ethanol conversion at lower contact time. An interesting effect observed at high zirconium loadings was an unexpectedly selectivity towards butenes, as high as 25%, when compared to other zirconium-based catalysts [16,32,69]. The ratio of ethanol/acetaldehyde had a significant influence on the formation of butenes. As shown on Figure 12, for the catalyst 2% $Zr/SiO_2$ at 593 K and WHSV of 1.2 $h^{-1}$, the selectivity towards butenes was higher than that of butadiene at high acetaldehyde content. At high ethanol content, the formation of BD increases. Interestingly, while the C4 yield (butadiene + butane) remains high under these various conditions, ethylene formation remained low. Although the authors do not speculate on the origin of the butenes species, it has been reported that butenes are not formed by hydrogenation of butadiene [16]. This would mean that sol-gel prepared $ZrO_2$ has some degree of activity in the Guerbet reaction and butenes are formed by the dehydration of 1-butanol or that some other pathway is involved. Alkali-doped $ZrO_2/SiO_2$ has been reported as active in the Guerbet reaction, however it is unlikely that an acidic material would preferably hydrogenate crotyl alcohol rather than dehydrate it without the presence of a dopant to suppress the acidity [21,81]. Because $ZrO_2$ is known for being amphoteric, the authors suggest that the great degree of dispersion together with interaction with the silica phase might have altered the acid-base properties of the oxide. Regardless of the explanation, at sufficient ethanol content in the feed, BD production was reasonable. The authors conclude that 2 wt % is an appropriate amount of $ZrO_2$ for the sol-gel synthesis, beyond which undesired active sites may be formed despite the metal's dispersion. The optimal catalysts, recorded at 593 K for a WHSV of 1.8 $h^{-1}$ and a EtOH/AA ratio of 3.5 had a butadiene yield of 31.6% for a productivity of 0.33 $g_{BD} \cdot g_{cat}^{-1} \cdot h^{-1}$ after 3 h on stream (ID: 21 in Figures 15 and 16).
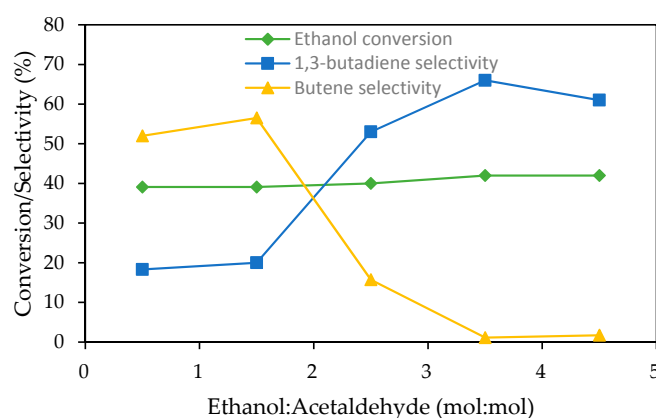


**Figure 12.** Effect of ethanol/acetaldehyde ratio in the feed over 2% $Zr/SiO_2$ (*T* = 593 K, *WHSV* = 1.2 $h^{-1}$). Reprinted with permission from [35]. Copyright 2015, Royal Society of Chemistry.

Lee et al. used a connected double fixed reactor system with dedicated functionalities to achieve high butadiene production from ethanol. In the first reactor, a gaseous ethanol feed was converted over a copper-containing catalyst [36]. The second reactor was packed with zirconium-containing catalyst to convert the resulting ethanol-acetaldehyde mixture to butadiene. Both metal oxides were highly dispersed over mesocellular silica foam (MCF), a silica support possessing high surface area, high mesoporosity and ultra large, interconnected nanopores. MCF was prepared according to the procedure disclosed in the literature [82]. To achieve high dispersion of copper oxide over silica, an ion-exchange method was used. Zirconium oxide was introduced into the support by urea hydrolysis. In both cases, drying and a calcination at 773 K for 3 h followed. These methods afforded 4.7% Cu/MCF and 2.7% Cu/MCF. XRD and scanning transmission electron microscopes combined with energy-dispersive X-ray spectroscopy (STEM-EDX) indicated a high degree of dispersion for both active phases. $N_2$ physisorption and the BET method revealed that the large surface area and porous volume were preserved despite the synthesis procedure. Different types of commercial silica were also used as support for zirconium for comparison. As the temperature of each reactor could be adjusted separately, the first reactor was fine-tuned so as to produce an optimal ethanol-to-acetaldehyde ratio to feed into the second reactor, which was also optimized to maximize butadiene formation. The addition of water in the ethanol feed is a convenient way to measure whether a process is suited for the transformation of crude bioethanol, which contains some amount of it. Lee et al. therefore tested the effects of including 10% water with the ethanol into the first reactor. In turn, the optimal ethanol-to-butadiene ratio varied between 0.69 and 1.68, and depended on the WHSV or the presence of water. The latter had the effect of reducing the optimal ethanol-to-acetaldehyde ratio, meaning acetaldehyde was actually the most abundant species in the feed. After careful optimization, a butadiene yield of 64.4% and productivity of 1.4 $g_{BD}\cdot g_{cat}^{-1}\cdot h^{-1}$ for a WHSV of 3.7 $h^{-1}$ after 15 h on stream was be obtained. The temperatures of the first and second reactors were respectively 523 and 673 K. In terms of productivity, these results are the highest found in the literature concerning the two-step process and the ethanol-to-butadiene conversion as a whole. Regarding the stability of this system, the high ethanol conversion and butadiene selectivity were slowly eroded over a period of tens of hours, but the system was successfully regenerated twice by heat treatment in air. Similarly to previously discussed publications, deactivation was attributed to coke formation. To explain the performances of their catalytic system, the authors argue that the high activity can attributed to the high dispersion of the metal oxides, while the large pores of the support help preventing mass-transfer issues and coking. This later conclusion is supported by the poor performances of catalysts supported on commercial silica, which lacks such morphological properties.

### 2.3. Other Catalytic Systems

Other Acid Catalysts

De Vos et al. have reported a novel silica-supported hafnium oxide mixed with zinc silicate catalyst yielding 68% butadiene with a productivity of 0.26 $g_{BD}\cdot g_{cat}^{-1}\cdot h^{-1}$ at 633 K with a WHSV of 0.64 $h^{-1}$ for a TOS of 10 h [37]. Remarkably, ethylene selectivity remained below 10% despite ethanol conversion nearing 100%. These results were achieved after making several modifications to a $Cu_xZn_yZr_zO_n/SiO_2$ catalyst first reported by Jones et al. [11]. Initially, zirconium was substituted by hafnium for its softer acid properties with the aim to reduce ethylene formation. Hafnium was introduced into silica by aqueous impregnation before calcination. Hafnium-containing catalysts were first reported as notably active in the Orstromislensky process by Corson et al. and were studied by Corson et al. and Jones et al. [11,41]. This first modification more than halved ethylene selectivity, but only slightly improved butadiene yield. The second modification involved mixing the silica-supported hafnium oxide with the zinc silicate hemimorphite as a substitute for copper and zinc. Hemimorphite was previously reported to catalyze the addition of methanol to propene through the $Zn^{2+}$ open sites found on its surface. The zinc silicate proved to be highly active in the formation of

acetaldehyde, but also to increase butadiene selectivity at the expense of ethylene when combined with Hf/SiO$_2$. Hemimorphite alone did not produce any butadiene. The increased activity is attributed to synergy between hafnium(IV) and hemimorphite resulting in the near disappearance of Brønsted acid sites, as measured by pyridine-FTIR and the activity of the zinc silicate in the dehydrogenation of ethanol. A notable feature of this catalyst is the importance of the synthesis method; to be fully active, hemimorphite had to be mixed in water with Hf/SiO$_2$ at room temperature, followed by calcination. All other approaches involving either reflux conditions or impregnation of hemimorphite with hafnium resulted in poorly active materials.

The activity of tantalum oxide was demonstrated by Corson et al. during the Second World War. Copper-doped silica-supported tantalum oxide was shown to be amongst the most active catalysts for the one-step conversion of ethanol [41]. In 2014, Chae et al. showed tantalum-containing ordered mesoporous silica were highly active for the two-step process [47]. More recently, Kyriienko et al. have reported the high selectivity of a tantalum-modified zeolite beta catalyst for the two-step process [38]. Tantalum(V)-single sites BEA zeolites were synthesized by 2-step post-synthesis method similar to that used in other articles discussed in this work. Briefly, dealumination of BEA zeolite was conducted using nitric acid to produce vacant silanol sites. Impregnation with varying amounts of tantalum ethoxide followed, affording samples believed to contain 1 and 3 wt % tantalum. The acid and basic properties of the modified zeolites were characterized by pyridine, pyrrol and CDCl$_3$-FTIR. These techniques suggested the presence of Lewis acid sites, and medium and weak basic sites. An absence of signals usually assigned to Brønsted acid sites was noted. With an ethanol feed alone, 1% Ta/BEA was active for the conversion of ethanol to butadiene. Selectivity towards butadiene at 623 K and WHSV of 0.8 h$^{-1}$ was 28.9%. Acetaldehyde was also produced in notable amounts, attributable to the redox properties of Ta(V) [83]. Dehydration products were also generated in significant amounts. Higher Ta(V) content increased the formation of ethylene, a phenomenon the authors explain by the formation of closed tantalum sites bound to four silicon atoms, as described by Ivanova et al. in the case of Zr/BEA, which are believed to be less active in the formation of butadiene [49,70]. With an ethanol/acetaldehyde mixture, the catalysts proved to be much more selective towards the desired product. At 623 K, with an EtOH/AA ratio of 3.7 and for a WHSV of 0.8 h$^{-1}$, butadiene yield for 3% Ta/BEA was 43.1% after 4 h on stream with a productivity of 0.20 g$_{BD}$·g$_{cat}^{-1}$·h$^{-1}$. The authors argued that the system lacked redox properties for the dehydrogenation of ethanol, as acid-base properties are believed to be predominant over redox properties in the case of Ta/BEA materials.

Supported niobium oxide can possess redox and acidic properties depending on the nature of the support [84–86]. Niobium oxide was identified as active for the two-step process by Toussaint et al. in 1947 [48]. Ivanova et al. have reiterated this claim, adding that niobium—amongst other metals—could be used to produce butadiene from ethanol when properly promoted [53]. Kyriienko et al. have investigated niobium-modified zeolite BEA for the ETB reaction [39]. This was done in the context of a study on the effects of the metal's incorporation with the zeolite framework state on a gas- and liquid-phase tandem process. The catalysts were prepared in a two-step post-synthesis method: dealumination of BEA was conducted using nitric acid; niobium ions were introduced into T-vacant sites by impregnation using niobium ethoxide as precursor. Washing with deionized water, drying and calcination at 723 K for three hours followed these procedures. Samples containing 0.7 and 2.0 wt % were prepared in this manner. The mononuclear incorporation of Nb(V) into the zeolite framework for the 0.7% Nb/BEA was demonstrated using XRD, DR UV–Vis, MAS NMR and FTIR. 2.0% Nb/BEA was shown to possess both the mononuclear species—albeit in lower amounts—and extra-framework octahedral niobium oxide. Notably, the presence of polynuclear species was evidenced by the presence of specific signals on the DR UV–Vis spectrum. In terms of surface properties, pyridine-FTIR revealed the presence of mostly weak Lewis acid sites, with some medium and strong sites, on both samples. Di-*tert*-butyl pyridine-FTIR further indicated the presence of very weak Brønsted on the surface of the catalyst that could not detected with pyridine. Higher ethanol conversion, TOF and butadiene yield were observed on 0.7% Nb/BEA. However, ethylene

and diethyl ether yields were also higher. In fact, the combined selectivity towards both dehydration products was higher than the sum of those presumably resulting from the dehydrogenation route. Evidently, mononuclear Nb(V) species are more active for all reactions and side-reactions involved in the Lebedev process than extra-framework species. Nevertheless, the catalytic performance of Nb/BEA in the one-step process was under average when compared to many of the recent materials reported in the literature [7,29]. As with Ta/BEA discussed above, this phenomenon could be attributed to the lack of the redox properties or modification to suppress ethanol dehydration. The addition of acetaldehyde in the feed at an ethanol-to-acetaldehyde ratio of 2.7 further evidenced the better activity of mononuclear species, as all measures of activity (ethanol conversion, butadiene and ethylene yields) were higher despite lower metal content. At 623 K, with an EtOH/AA ratio of 2.7 and for a WHSV of 0.8 h$^{-1}$, butadiene yield over 0.7% Nb/BEA was of 23.6, for a productivity of 0.11 g$_{BD}$·g$_{cat}^{-1}$·h$^{-1}$. Despite the increase in performances from the addition of acetaldehyde, the performances of Nb/BEA remains poorer than similar Ta and Zr-containing catalysts, reconfirming a trend previously observed by Toussaint et al. (referred to by its former name columbium in their article) [38,48,69]. For this reason, it is improbable that niobium could be used as a viable substitute to zirconium or other Lewis solid acids.

La-Salvia et al. report the catalytic activity of acidic Al-MCM-41 modified with chromium and barium for the one-step conversion of ethanol to butadiene. MCM-41 is an ordered mesoporous silica with large surface area. Acidity was generated by the introduction of an aluminium precursor in the preparation procedure. The as-synthesized Al-MCM-41 was sequentially doped using barium and chromium IWI method. It was argued that barium would provide the acidic material with basic properties, while chromium would promote the ethanol dehydrogenation. Unmodified Al-MCM-41 was also kept for characterization and catalytic testing. As in the work of Sels et al., the ordered nature and structure of Al-MCM-41 did not survive the impregnation process. Powdered XRD and N$_2$ physisorption revealed the progressive collapse of Al-MCM-41 framework with each impregnation. Additionally, amorphous barium silicate was detected and supposed to block pore access. Although chromium oxide was not detected by XRD, changes in surface chemical properties suggest it was present as highly dispersed particles. CO$_2$ chemisorption indicated a progressive increase in the density of basic sites after the addition of each dopant–first barium, then chromium. In terms of activity, Al-MCM-41 and 16% Ba/Al-MCM-41 were highly active for the dehydration of ethanol. No butadiene was observed and acetaldehyde was exclusively detected in small amount over the barium-containing catalyst. The acidity of Al-MCM-41 is well established and the likely cause of the significant ethanol dehydration observed [87]. This suggests that the alkali nature of barium was either insufficient to curb this acidity or that the framework collapse reduced the accessibility to the barium-containing surface. The subsequent introduction of chromium greatly improved the activity of material. At 723 K for a WHSV of 3.07 h$^{-1}$, 1.4% Cr-16% Ba/Al-MCM-41 had a butadiene yield of 22.1% and a productivity of 0.40 g$_{BD}$·g$_{cat}^{-1}$·h$^{-1}$ after 10 h on stream, along with a significant increase in acetaldehyde selectivity. The role of Cr$_2$O$_3$ as promoter of ethanol dehydrogenation in the ETB reaction has been previously reported and is the likely reason for the increased production of butadiene [8,41]. As the activity of Cr/MCM-41 was not reported, it is difficult to the role of barium in this improvement or if Ba and Cr had any synergic contribution in that regard. It should be noted that chromium-containing amphoteric mixed oxides were reported as active for the ETB reaction, but not silica-supported Cr$_2$O$_3$, evidencing some contribution from MCM-41 and/or Ba [26,41]. A decrease in ethanol conversion is observed over a period of 24 h. Coke formation on the catalytic surface, evidenced by thermal gravimetric analysis, is the likely cause of this deactivation. So far, MCM-41 has proved to be a poor support for materials active in the conversion of ethanol to butadiene.

Palkovits et al. have approached the synthesis of butadiene from ethanol with a two-stage system. An ethanol/acetaldehyde mixture with a ratio of 4 was obtained during the first stage of the process. The second step concerned the conversion of this mixture to butadiene over modified zeolite BEA catalysts. Two catalysts were tested for the dehydrogenation of ethanol: Cu/SiO$_2$ and

Ag/SiO$_2$ prepared by IWI. Although only the copper catalyst was reduced under hydrogen flow, subsequent catalytic test of CuO/SiO$_2$ coupled with post-reaction characterization revealed that both silver and copper are readily reduced under an ethanol flow at the reaction temperature [50]. EtOH/AA ratio of 4 (20% acetaldehyde yield) was obtained over Cu/SiO$_2$ at 463 K and WHSV of 0.24 h$^{-1}$ and remained highly stable over a period of 90 h on stream. No other product except acetaldehyde could be detected. On the contrary, Ag/SiO$_2$ suffered from deactivation in the first 20 h on stream before stabilizing. Furthermore, small quantities of side-products were detected, not unlike the observations of Ivanova et al. on similar a Ag/SiO$_2$ catalyst [59]. Because of its obvious benefits, Cu/SiO$_2$ was selected for the first stage of this process. The second stage of the process concerned the conversion of the ethanol/acetaldehyde feed to butadiene at 573 K. Palkovits et al. studied the relation between the acid and basic properties of modified zeolite BEA and the their catalytic activity. To change the acidity and basicity of the catalysts, the acidic zeolites with varied Al/Si ratios underwent several modifications: the acidity of the zeolites was passivated by the exchanging alkaline and earth alkaline ions (Ca$^{2+}$, K$^+$ and Cs$^+$) with the surface protons; basicity was introduced by impregnating the zeolites and alkali-modified zeolites with magnesium oxide; these magnesium-modified zeolites were further modified by the addition of different metal oxides (Al$_2$O$_3$, ZnO and NiO). The catalytic activity of these materials was evaluated at the ethanol/acetaldehyde ratio obtained previously and compared with their acid-base properties measured by NH$_3$ and CO$_2$-TPD respectively; the acid-based properties was represented by a ratio between the number of acid and basic sites, $n_{\text{acidic}}/n_{\text{baisc}}$. From this comparison, a correlation between the balance of acid and basic sites with the catalytic activity was obtained (Figure 13). Butadiene selectivity was correlated with a balance between the number of basic and acid sites at ratios approximating 1 (Figure 13A). However, it had to be achieved by the introduction of basic functions with MgO; passivation with alkali metals alone suppressed ethanol conversion, barely improving BD selectivity. On the contrary, selectivity towards dehydration products (ethylene and diethyl ether) was associated with an excess of acidity, expressed by a $n_{\text{acidic}}/n_{\text{baisc}}$ ratio above 1 (Figure 13B). The ethanol conversion rate followed a similar trend, evidently the result of increased ethanol dehydration (Figure 13C). Based on these observations, the authors conclude that a balance between the acid and basic properties is essential. However, the correlations obtained did not distinguish between the nature and strength of the active and basic sites, therefore not providing an accurate assessment of the necessary properties to catalyze the reaction. Pyridine-FTIR indicated the presence of Brønsted acid sites on the zeolites with smaller Si/Al ratio, while greater Si/Al ratio materials displayed mostly signals for Lewis acid sites. Regardless of the type of acidity, ethylene selectivity remained above 88%, evidencing the necessity of additional chemical properties. The combination of MgO with alkali metals proved relatively successful, where it increased BD selectivity while maintaining a high ethanol conversion, suggesting that basic active sites are responsible for the production of acetaldehyde. Ultimately, the optimal catalyst was obtained by the introduction of basic MgO and further modified with ZnO to promote ethanol dehydrogenation. At 573 K, with a EtOH/AA ratio of 4 and for a GHSV of 96.0 h$^{-1}$, ZnO-MgO/BEA showed a BD yield of 33% butadiene. Due to a lack of reaction detail, it is difficult to compare these performances to other catalysts.
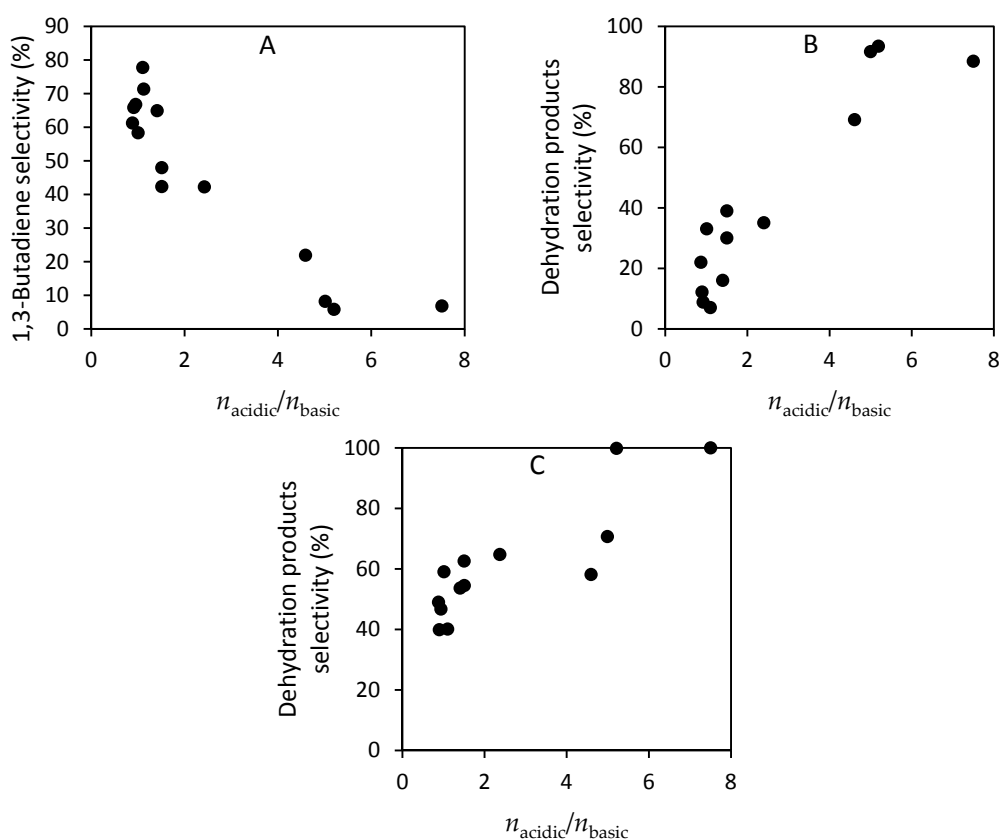
**Figure 13.** Correlation curves between the ratio between the number of acid and basic sites with: (**A**) 1,3-butadiene selectivity; (**B**) dehydration products selectivity; (**C**) ethanol conversion. Reprinted with permission from [60]. Copyright 2015, Elsevier.

## 3. Discussion

The production of 1,3-butadiene from renewable sources could address the sustainability issues associated with steam cracker extraction, the current method of choice. One such production process is the catalytic conversion of ethanol to 1,3-butadiene. The main advantage of this process is that it has successfully been implemented decades ago, before the petroleum based route. Some studies have already suggest that the one or two-step process could soon [3,6,43]. Industrial initiatives such as the Michelin project Biobutterfly suggest that biosourced butadiene is a possibility [88]. Accordingly, research on the subject has undergone a renaissance in the past few years: catalytic systems first discovered decades ago are being retested, new catalysts are being developed and the number of publications on the subject is growing at a considerable rate. The latest scientific investigations have focused on increasing the performances of catalytic materials either for the one-step or two-step process with the aim of improving their economic viability. A crucial target for improvement has been the productivity in butadiene, but also the reduction of non-recyclable byproducts. It is understood that catalytic activity requires a combination of either acid, basic and redox properties—the balance is thought to be the key to achieve high productivity. With each catalytic system also comes the use of various promoters to alter this balance or to introduce new functionalities, incidentally adding a new layer of complexity to the preparation of catalysts. Although significant progress has been made, aspects crucial to the rational design of new catalysts, namely the exact nature of some active sites, the true reaction mechanism and the optimal preparation methods have either not yet been fully elucidated or are still under debates. To solve this issue, researchers have sought to understand the relation between the chemical and structural properties of material and its catalytic activity—with various degrees of success. As highlighted by Sels et al. concerning MgO-SiO$_2$, a lack of "systematic

studies with advanced surface characterization tools in combination with catalytic measurements" has plagued the development and understanding of ETB reaction [8]. This review has highlighted the recent progress achieved in this field.

The issue with designing catalysts for the ethanol-to-butadiene reaction lies in the complexity of the reaction mechanism which requires different active sites. Because the chemical and structural properties that give rise to the catalytic activity are not fully understood, it becomes difficult to generate or balance these properties in a way that maximizes butadiene production. Only by systematic studies with advanced surface characterization tools in combination with catalytic measurements this issue might be resolved [8]. One such study can be found in the case of the Ag/Zr/BEA catalysts developed by Ivanova et al. in which a new highly active catalytic system for the Lebedev process was devised, carefully characterized until an active site could be identified, then rationally optimized (Figure 14). The first step of the development involved identifying and combining the chemical properties known to partake in the ethanol conversion to BD. While the activity of silica-supported $ZrO_2$ in the two-step process due to its Lewis acidity had been established decades before, it lacks the properties necessary to catalyze the first step of the Lebedev process [41,67]. This issue was resolved by the addition of silver which can dehydrogenate ethanol without an oxidant when supported on silica [58]. By combining both properties, a new catalytic system was created and proven to be superior to the combination of other metals and metal oxides—according to their patent [53]. The next step was to understand the relation between the chemical properties of the catalyst and its activity. Thus, both the activity of silver in the production of acetaldehyde, and of zirconium oxide in the MPVO reduction and acetaldehyde condensation were investigated [59,68]. The effect of the support on the activity of the catalyst was also investigated, which indicated that molecular sieves allowing for larger dispersion of the active phase increased the performance of the catalyst [69]. Zeolite BEA became the support of choice. Finally, an active site was recognized through a sequential chemisorption of $CDCl_3$ and CO measured by FTIR spectroscopy. This method allowed the distinction between closed and open Lewis acid sites within the zeolite framework; the latter was linearly correlated with butadiene formation. Ivanova et al. followed with the optimization of their catalysts by intentionally inducing the now-identified active sites. This was achieved using a novel method which involved the mixture of DMSO-dissolved $ZrOCl_2$ with dealuminated zeolite BEA under reflux conditions. It was suggested that the solvent prevented the aggregation of zirconium oxide, allowing the formation of isolated ion sites, while steric hindrance, diffusion limitations or energetic limitations were thought to cause of the preferential grafting as open Zr sites. With the addition of silver to Zr/BEA, one of the most productive catalysts was obtained. Although some subsequently reported catalysts were found to be more productive than Ag/Zr/BEA, their superiority is attributed to the use of new materials, not out of rational design. By systematically studying these materials, new and better catalytic systems could be devised.
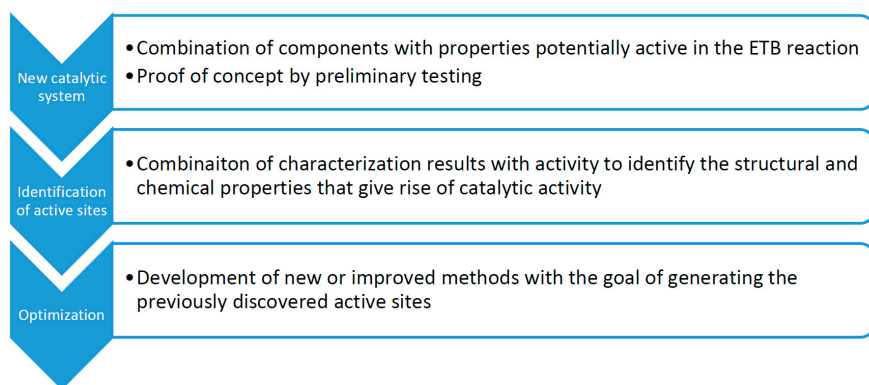


**Figure 14.** Development progress of Ag/Zr/BEA as exemplified by Ivanova et al.

Despite being the most investigated catalyst, the magnesia-silica system is still at the stage of pin-pointing the chemical and structural properties from which originates their activity. One issue is the difference in preparation method which significantly alters many of the features of the MgO-SiO$_2$ catalysts, making their comparison difficult, as evidenced by the different Mg-to-Si ratios being reported as optimal. In general, it is recognizes that a predominantly basic catalyst with some degree of acidity is the preferred balance to produce active materials [7,13,25,27,29,30,51]. Weckhuysen et al. have reported that sufficient amount of Lewis acid in the form of Mg–O–Si with small amounts of strong basic sites has led to the most active wet-kneaded catalysts [51]. They also concluded that a cooperation between acid and basic sites was involved in the condensation of acetaldehyde. Sels et al. have proposed that the strong basic sites present in the form of O$^{2-}$ defects in the magnesia, while uncoordinated Mg(II) cations isolated in silica could participate in the dehydration reactions and MPVO reduction [29]. In the context of their mechanism, Cavani et al. have suggested that the reaction of acetaldehyde with the carbanion would occur on defects and edges of the MgO phase, while the dehydration of crotyl alcohol into butadiene would occur with Mg–O–Si Lewis acid sites transformed into Brønsted acid sites in the presence of water [13]. The most interesting observation has been that of Weckhuysen et al. concerning the activity of magnesium silicates [27]. Using $^1$H-$^{29}$Si CP MAS-SSNMR, correlation between the relative amount of layered hydrous magnesium silicates formed during the interaction between magnesia and silica was linearly correlated with butadiene yield, while the relative amount of hydrous amorphous magnesium silicate was correlated with ethylene formation. Although additional characterization is required to clarify their properties and exact role in the reaction, it remains the first instance of a structural property being directly correlated with catalytic activity that could mark a beginning of rationally designed MgO-SiO$_2$ catalysts. Coincidently, Baba et al. investigated the activity of layered hydrous magnesium silicate-talc [19]. The team reported that synthetic talc alone did not lead to butadiene; however, it was found to be the most active catalyst after zinc was incorporated in the crystal lattice. A thorough investigation revealed that zinc did not promote any of the reaction steps besides ethanol dehydrogenation, suggesting talc alone was responsible for the high butadiene yield. Talc is an amphoteric material with proximate acid and basic sites, which are required to catalyze the ETB reaction, minus ethanol dehydrogenation [27]. It is possible that the active sites in MgO-SiO$_2$ system are the layered magnesium silicates with MgO providing the redox properties. In such case, the necessity of MgO and SiO$_2$ is dubious, as redox properties can more easily be introduced in talc with the use of dedicated promoters. The recent investigations on MgO-SiO$_2$ catalytic system indicate a shift away from characterization studies to the new preparation methods capable of generating active sites. Already, wet-kneading spherical silica with MgO particles and mechano-chemical mixing have been reported to generate layered magnesium oxides, which is active in the ETB reaction [3,27,28].

In the past few years, several materials, old and new, have been tested for either the one or two-step process, giving rise to new opportunities for the design of catalytic systems. For instance, many promoters of the nonoxidative dehydrogenation of ethanol to acetaldehyde have successfully been implemented in various catalytic systems. Metals such as gold, copper and silver have been used in the MgO-SiO$_2$ catalytic system and others. In the case of Cu/MgO-SiO$_2$, it was found that Cu disperses more readily on the magnesia phase than on silica, affecting its activity, while the opposite was true for Ag [29,50]. The introduction of Cu lead to a slow deactivation of the catalyst by coke formation that did not occur on the unpromoted catalyst. The catalytic activity of Au/MgO-SiO$_2$ was reportedly inferior to that of the other metals, but it is possible that the synthesis method, which led to the formation of amorphous magnesium silicate previously associated with ethylene formation, indivertibly lowered the selectivity towards butadiene. Measuring the activity of gold-modified catalyst without such phase could shed some light on this issue. Silica-supported Cu and Ag where also used as catalysts for the formation of acetaldehyde in the first step of the Ostromislensky process [36,60]. Of the two metals, copper was found to be the highly selective and stable, while silver deactivated and generated some amounts of byproducts [60]. It should be noted

however, that the loading of silver was of almost 10%, whereas the literature indicates that high metal loading is detrimental, recommending 5% instead [58]. Finally, metal promoters have been reported to be successfully reduced in situ by ethanol, potentially making a pre-treatment with hydrogen optional [32,50,60].

Zinc oxide was also used as promoter for the dehydrogenation of ethanol. It proved to greatly increase the activity of MgO-SiO$_2$ adding some Lewis acidity by interacting with silica [31]. Zinc oxide was also used to balance the acid properties of hard-templated ZrO$_2$ and silica-supported ZrO$_2$ while also providing the missing redox properties to the Lewis acidic materials [33,37]. The use of hemimorphite, a zinc silicate, combined with a silica-supported Lewis acid resulted in a highly selective catalyst; it simultaneously promoted the dehydrogenation of ethanol, reaching 100% ethanol conversion, while passivating the Brønsted acidity of the metal oxide, significantly lowering ethylene selectivity [37]. Although in the latter case, the specific origin of the high activity has not been identified, it appears that zinc-based promoters have the double effect of improving the redox properties of material, while also altering its acid properties to a greater extent than metal promoters.

Rather than tweaking the preparation method, the acid properties of a catalyst can be altered by a post-treatment with alkali metals [30,33,60]. Both Jones et al. and Wang et al. have reported the selective poisoning of the stronger acid sites on their zirconium-containing catalysts [30,33]. As a result, ethylene formation was significantly suppressed, boosting butadiene and acetaldehyde selectivity. Because acetaldehyde can be recycled and fed in the reactor again, alkali poisoning offers the opportunity of reducing the number of secondary products over acid-based catalysts. However, the poor results obtained with BEA-support alkali metals suggest that despite their basic properties, they do not participate as active sites in the ETB reaction [60].

The current study of Lewis acid catalysts discussed above has mostly focused on zirconium-containing materials, either supported on silica or a molecular sieve, but also as hard-templated bulk oxide [16,32,69]. However, several alternatives have been recently investigated. Originally evaluated together with zirconium decades ago, tantalum and niobium oxide have been revisited by Kyriienko et al., this time supported on zeolite BEA [38,39,48,67]. Both were found to lack the redox properties required to be active in the one-step process, but were reasonably active in the two-step process. Of the two, tantalum was found to be superior in activity and its productivity rivaled that of other zirconium catalysts tested in similar conditions [35]. On the contrary, niobium oxide could not be properly dispersed and displayed relatively poorer performances. These observations are in accord with a trend noted by Toussaint et al. concerning the activity of the three Lewis acids [48]. The substitution of zirconium by hafnium as the Lewis acid component of a catalyst resulted in a reduction of ethylene formation, while preserving a similar yield of butadiene [37]. This phenomenon was attributed to the softer acid properties of hafnium. When combined with hemimorphite, it proved to be a highly selective catalyst with high conversion rate. Hafnium offers the possibility of designing Lewis acid catalysts with lower selectivity towards dehydration products.

A recent publication by Kyriienko et al. suggest that lanthanum oxide may possess the basic properties required to catalyze the ETB reaction [34]. Their La-Zn-(Zr)-Si catalyst proved to be one of the most productive catalysts in the one-step process with stability up to 10 h. The combination of these oxides was argued to provide the redox, acid and basic properties required to catalyze the reaction. According to the authors, zinc oxide provided the redox properties, zirconium oxide the Lewis acidity and lanthanum oxide the basic properties. New opportunities could arise from this discovery, as lanthanum could be used to provide basicity to other catalytic systems.

The importance of the support was also highlighted in the reviewed literature. The most active catalyst was obtained by dispersing zirconium oxide over mesocellular silica foam [36]. The performance of this catalyst was attributed to the high degree of dispersion of ZrO$_2$ enabled by the great surface area of the support, and to the large, interconnect mesopores of MCF, which diminish the formation of coke and issues relating to the mass-transfer of reagents into the catalyst. Incidentally, the use of an incorrect support resulted in undesired properties. In particular, MCM-41 was shown to be

a poor support, as it structural integrity was repeatedly compromised by post-synthetic modifications, once as silica source for an $MgO$-$SiO_2$ catalyst, another time as an acidic support for $Cr_2O_3$ and $BaO_2$ [7,40]. In both case, the ordered mesoporous structure of the silicate was lost.

## 4. Conclusions

In this paper, the latest advances in the design of catalytic systems for the ethanol-to-butadiene reaction have been reviewed. The use of new components, as wells as a careful optimization of existing catalysts have allowed scientists to surpass the performances of previous catalytic systems. In particular, the productivity of butadiene under realistic industrial conditions (with large ethanol flow) has seen a dramatic increase in both one and two-step process [7]. Figure 15 gives a visual representation of the most productive catalysts reported in recent years. Considering that a large proportion of the numerous catalysts developed over the last decades could not reach a productivity of 0.150 $g_{BD} \cdot g_{cat}^{-1} \cdot h^{-1}$ (suggested as Jones et al. in 2012 as the minimum for industrial application), it illustrates the progress in ETB reaction.
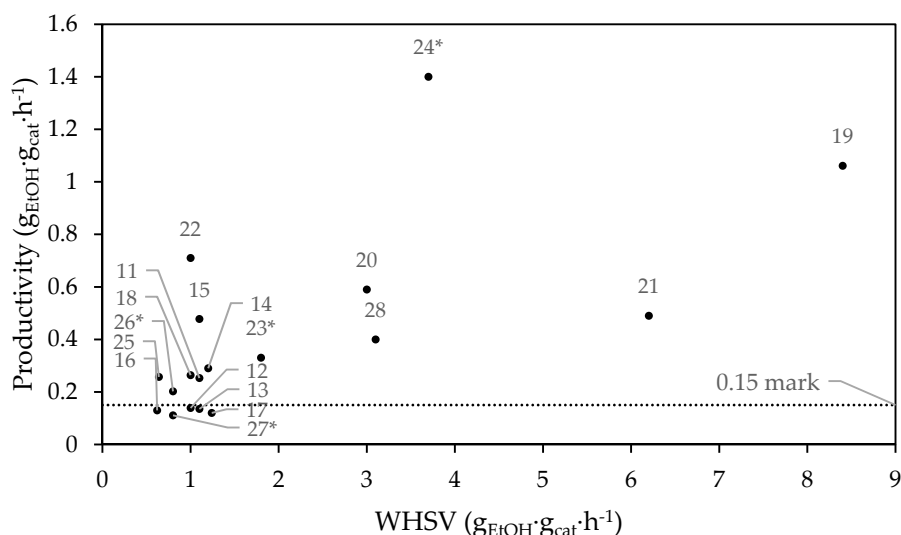


**Figure 15.** 1,3-Butadiene production versus weight hourly space velocity (WHSV) for the reviewed catalysts in reference to the ID number in Table 1. * indicates a result obtained from a two-step process.

Comparing Figure 16 below with a similar figure (Figure 14) found in the book chapter by Cavani et al. on this subject representing the performances in terms of yield of selected catalysts shows that the past 2 to 3 years have afforded as many highly active catalysts as the past 70 years combined [14]. This progress was accomplished both by the rational design of new catalytic systems, as well as the use of highly active new components, such as lanthanum oxide or mesoporous silica foam for the support of zirconium oxide. As illustrated, the majority of the catalysts showed a BD yield between 20% and 40%, which is in line with the performances reported in the literature. Nevertheless, several catalysts were able to go beyond, with two catalysts reaching values above 60%. Only the notorious catalyst be Ohnishi et al. and one catalyst Ivanova et al. had been reported to reach that point [14].
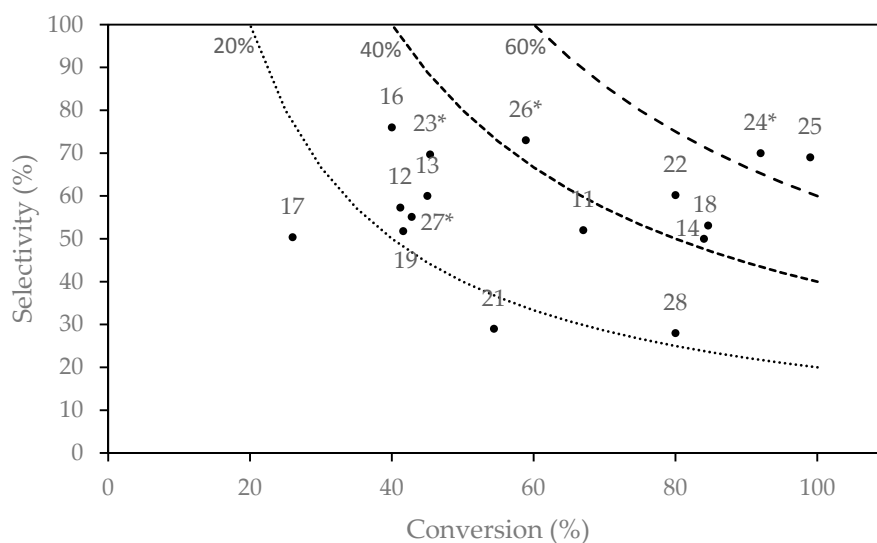
**Figure 16.** 1,3-Butadiene selectivity versus ethanol conversion for the reviewed catalysts in reference to the ID number in Table 1. * indicates a result obtained from a two-step process.

Many aspects of the ETB reaction still necessitate investigation. Obviously, settling the question of the reaction mechanism is a primordial objective, as is the establishment of clear link between certain properties and BD productivity; the identification of the active sites of each catalytic systems would enable a more rational design of new active materials. Another issue that has yet to be fully addressed is the effect of water in the system, as it would help predict the viability of using more affordable unpurified bioethenol. Already Cavani et al. have observed that additional water in the feed leads to the formation of new Brønsted acid sites from existing Lewis sites [13]. Lee et al. have also noted that the presence of water increases the need for acetaldehyde in the feed of the two-step process [36]. Another aspect that will grow in importance is the too-often ignored time-on-stream stability of the catalytic materials. Currently, it is believed the coke deposition is the principal source of deactivation [36,40,50,54]. As the performances of the catalysts improve, growing attention will be devoted to minimizing this phenomenon. With the old & new chemistry of the ETB reaction being currently investigated by several research teams, it is likely that the issues will be addressed in the near future and a transition from the laboratory to the industry scale is maybe now just a question of time.

**Author Contributions:** Guillaume Pomalaza wrote the paper; Franck Dumeignil, Vitaly Ordomsky and Mickaël Capron revised the paper.

**Conflicts of Interest:** The authors declare no conflict of interest.

## References

1. Ouhadi, T.; Abdou-Sabet, S.; Wussow, H.-G.; Ryan, L.M.; Plummer, L.; Baumann, F.E.; Lohmar, J.; Vermeire, H.F.; Malet, F.L.G. Thermoplastic elastomers. In *Ullmann's Encyclopedia of Industrial Chemistry*; Wiley-VCH Verlag GmbH & Co. KGaA: Weinheim, Germany, 2014; pp. 1–41.
2. Dahlmann, M.; Grub, J.; Löser, E. Butadiene. In *Ullmann's Encyclopedia of Industrial Chemistry*; Wiley-VCH Verlag GmbH & Co. KGaA: Weinheim, Germany, 2011; Vol. 100 C, pp. 1–24.
3. Shylesh, S.; Gokhale, A.A.; Scown, C.D.; Kim, D.; Ho, C.R.; Bell, A.T. From sugars to wheels: The conversion of ethanol to 1,3-butadiene over metal-promoted magnesia-silicate catalysts. *ChemSusChem* **2016**, *9*, 1462–1472. [CrossRef] [PubMed]
4. Ezinkwo, G.O.; Tretyakov, V.P.; Aliyu, A.; Ilolov, A.M. Fundamental issues of catalytic conversion of bio-ethanol into butadiene. *ChemBioEng Rev.* **2014**, *1*, 194–203. [CrossRef]

5. Sun, J.; Wang, Y. Recent advances in catalytic conversion of ethanol to chemicals. *ACS Catal.* **2014**, *4*, 1078–1090. [CrossRef]

6. Burla, J.; Fehnel, R.; Louie, P.; Terpeluk, P. Two-Step Production of 1,3-Butadiene from Ethanol. Available online: http://repository.upenn.edu/cgi/viewcontent.cgi?article=1033&context=cbe_sdr (accessed on 12 December 2016).

7. Makshina, E.V.; Janssens, W.; Sels, B.F.; Jacobs, P.A. Catalytic study of the conversion of ethanol into 1,3-butadiene. *Catal. Today* **2012**, *198*, 338–344. [CrossRef]

8. Makshina, E.V.; Dusselier, M.; Janssens, W.; Degrève, J.; Jacobs, P.A.; Sels, B.F. Review of old chemistry and new catalytic advances in the on-purpose synthesis of butadiene. *Chem. Soc. Rev.* **2014**, *43*, 7917–7953. [CrossRef] [PubMed]

9. Angelici, C.; Weckhuysen, B.M.; Bruijnincx, P.C.A. Chemocatalytic conversion of ethanol into butadiene and other bulk chemicals. *ChemSusChem* **2013**, *6*, 1595–1614. [CrossRef] [PubMed]

10. Jones, M. Catalytic transformation of ethanol into 1,3-butadiene. *Chem. Cent. J.* **2014**. [CrossRef] [PubMed]

11. Jones, M.; Keir, C.; Iulio, C.; Robertson, R.; Williams, C.; Apperley, D. Investigations into the conversion of ethanol into 1,3-butadiene. *Catal. Sci. Technol.* **2011**, *1*, 267–272. [CrossRef]

12. Chieregato, A.; Velasquez Ochoa, J.; Bandinelli, C.; Fornasari, G.; Cavani, F.; Mella, M. On the chemistry of ethanol on basic oxides: Revising mechanisms and intermediates in the Lebedev and Guerbet reactions. *ChemSusChem* **2015**, *8*, 377–388. [CrossRef] [PubMed]

13. Ochoa, J.V.; Bandinelli, C.; Vozniuk, O.; Chieregato, A.; Malmusi, A.; Recchi, C.; Cavani, F. An analysis of the chemical, physical and reactivity features of MgO–SiO$_2$ catalysts for butadiene synthesis with the Lebedev process. *Green Chem.* **2016**, *18*, 1653–1663. [CrossRef]

14. Chieregato, A.; Ochoa, J.V.; Cavani, F. Olefins from biomass. In *Chemicals and Fuels from Bio-Based Building Blocks*; Wiley-VCH Verlag GmbH & Co. KGaA: Weinheim, Germany, 2016; pp. 1–32.

15. Jones, H.E.; Stahly, E.E.; Corson, B.B. Butadiene from ethanol. reaction mechanism. *J. Am. Chem. Soc.* **1949**, *71*, 1822–1828. [CrossRef]

16. Sushkevich, V.L.; Ivanova, I.I.; Ordomsky, V.V.; Taarning, E. Design of a metal-promoted oxide catalyst for the selective synthesis of butadiene from ethanol. *ChemSusChem* **2014**, *7*, 2527–2536. [CrossRef] [PubMed]

17. Gao, M.; Liu, Z.; Zhang, M.; Tong, L. Study on the mechanism of butadiene formation from ethanol. *Catal. Letters* **2014**, *144*, 2071–2079. [CrossRef]

18. Müller, P.; Burt, S.P.; Love, A.M.; McDermott, W.P.; Wolf, P.; Hermans, I. Mechanistic study on the Lewis acid catalyzed synthesis of 1,3-butadiene over Ta-BEA using modulated operando DRIFTS-MS. *ACS Catal.* **2016**, *6*, 6823–6832. [CrossRef]

19. Hayashi, Y.; Akiyama, S.; Miyaji, A.; Sekiguchi, Y.; Sakamoto, Y.; Shiga, A.; Koyama, T.; Motokura, K.; Baba, T. Experimental and computational studies of the roles of MgO and Zn in talc for the selective formation of 1,3-butadiene in the conversion of ethanol. *Phys. Chem. Chem. Phys.* **2016**, *18*, 25191–25209. [CrossRef] [PubMed]

20. Veibel, S.; Nielsen, J.I. On the mechanism of the Guerbet reaction. *Tetrahedron* **1967**, *23*, 1723–1733. [CrossRef]

21. Kozlowski, J.T.; Davis, R.J. Heterogeneous catalysts for the Guerbet coupling of alcohols. *ACS Catal.* **2013**, *3*, 1588–1600. [CrossRef]

22. Ho, C.R.; Shylesh, S.; Bell, A.T. Mechanism and kinetics of ethanol coupling to butanol over hydroxyapatite. *ACS Catal.* **2016**, *6*, 939–948. [CrossRef]

23. Scalbert, J.; Thibault-Starzyk, F.; Jacquot, R.; Morvan, D.; Meunier, F. Ethanol condensation to butanol at high temperatures over a basic heterogeneous catalyst: How relevant is acetaldehyde self-aldolization? *J. Catal.* **2014**, *311*, 28–32. [CrossRef]

24. Da Ros, S.; Jones, M.D.; Mattia, D.; Schwaab, M.; Barbosa-Coutinho, E.; Rabelo-Neto, R.C.; Bellot Noronha, F.; Carlos Pinto, J. Microkinetic analysis of ethanol to 1,3-butadiene reactions over MgO–SiO$_2$ catalysts based on characterization of experimental fluctuations. *Chem. Eng. J.* **2016**, *308*, 988–1000. [CrossRef]

25. Angelici, C.; Velthoen, M.E. Z.; Weckhuysen, B.M.; Bruijnincx, P.C. A. Effect of preparation method and CuO promotion in the conversion of ethanol into 1,3-butadiene over SiO$_2$–MgO catalysts. *ChemSusChem* **2014**, *7*, 2505–2515. [CrossRef] [PubMed]

26. Bhattacharyya, S.K.; Ganguly, N.D. One-step catalytic conversion of ethanol to butadiene in the fixed bed. II Binary- and ternary-oxide catalysts. *J. Appl. Chem.* **1962**, *12*, 105–110. [CrossRef]

27. Chung, S.-H.; Angelici, C.; Hinterding, S.O.M.; Weingarth, M.; Baldus, M.; Houben, K.; Weckhuysen, B.M.; Bruijnincx, P.C.A. On the role of magnesium silicates in wet-kneaded silica-magnesia catalysts for the Lebedev ethanol-to-butadiene process. *ACS Catal.* **2016**, *6*, 4034–4045. [CrossRef]

28. Larina, O.V.; Kyriienko, P.I.; Trachevskii, V.V.; Vlasenko, N.V.; Soloviev, S.O. Effect of mechanochemical treatment on acidic and catalytic properties of MgO–SiO$_2$ composition in the conversion of ethanol to 1,3-butadiene. *Theor. Exp. Chem.* **2016**, *51*, 387–393. [CrossRef]

29. Janssens, W.; Makshina, E.V.; Vanelderen, P.; De Clippel, F.; Houthoofd, K.; Kerkhofs, S.; Martens, J.A.; Jacobs, P.A.; Sels, B.F. Ternary Ag/MgO–SiO$_2$ catalysts for the conversion of ethanol into butadiene. *ChemSusChem* **2015**, *8*, 994–1008. [CrossRef] [PubMed]

30. Da Ros, S.; Jones, M.D.; Mattia, D.; Pinto, J.C.; Schwaab, M.; Noronha, F.B.; Kondrat, S.A.; Clarke, T.C.; Taylor, S.H. Ethanol to 1,3-butadiene conversion by using ZrZn-containing MgO/SiO$_2$ systems prepared by Co-precipitation and effect of catalyst acidity modification. *ChemCatChem* **2016**, *8*, 2376–2386. [CrossRef]

31. Larina, O.V.; Kyriienko, P.I.; Soloviev, S.O. Ethanol conversion to 1,3-butadiene on ZnO/MgO–SiO$_2$ catalysts: effect of ZnO content and MgO:SiO$_2$ ratio. *Catal. Lett.* **2015**, *145*, 1162–1168. [CrossRef]

32. Sushkevich, V.L.; Ivanova, I.I. Ag-promoted ZrBEA zeolites obtained by post-synthetic modification for conversion of ethanol to butadiene. *ChemSusChem* **2016**, *9*, 2216–2225. [CrossRef] [PubMed]

33. Baylon, R.A.L.; Sun, J.; Wang, Y. Conversion of ethanol to 1,3-butadiene over Na doped Zn$_x$Zr$_y$O$_z$ mixed metal oxides. *Catal. Today* **2014**, *259*, 446–452. [CrossRef]

34. Larina, O.V.; Kyriienko, P.I.; Soloviev, S.O. Effect of lanthanum in Zn-La(-Zr)-Si oxide compositions on their activity in the conversion of ethanol into 1,3-butadiene. *Theor. Exp. Chem.* **2016**, *52*, 51–56. [CrossRef]

35. Han, Z.; Li, X.; Zhang, M.; Liu, Z.; Gao, M. Sol–gel synthesis of ZrO$_2$–SiO$_2$ catalysts for the transformation of bioethanol and acetaldehyde into 1,3-butadiene. *RSC Adv.* **2015**, *5*, 103982–103988. [CrossRef]

36. Cheong, J.L.; Shao, Y.; Tan, S.J. R.; Li, X.; Zhang, Y.; Lee, S.S. Highly active and selective Zr/MCF catalyst for production of 1,3-butadiene from ethanol in a dual fixed bed reactor system. *ACS Sustain. Chem. Eng.* **2016**, *4*, 4887–4894. [CrossRef]

37. De Baerdemaeker, T.; Feyen, M.; Müller, U.; Yilmaz, B.; Xiao, F.S.; Zhang, W.; Yokoi, T.; Bao, X.; Gies, H.; De Vos, D.E. Bimetallic Zn and Hf on silica catalysts for the conversion of ethanol to 1,3-butadiene. *ACS Catal.* **2015**, *5*, 3393–3397. [CrossRef]

38. Kyriienko, P.I.; Larina, O.V.; Soloviev, S.O.; Orlyk, S.M.; Dzwigaj, S. High selectivity of TaSiBEA zeolite catalysts in 1,3-butadiene production from ethanol and acetaldehyde mixture. *Catal. Commun.* **2016**, *77*, 123–126. [CrossRef]

39. Kyriienko, P.I.; Larina, O.V.; Popovych, N.O.; Soloviev, S.O.; Millot, Y.; Dzwigaj, S. Effect of the niobium state on the properties of NbSiBEA as bifunctional catalysts for gas- and liquid-phase tandem processes. *J. Mol. Catal. A* **2016**, *424*, 27–36. [CrossRef]

40. La-Salvia, N.; Lovón-Quintana, J.J.; Valença, G.P. Vapor-phase catalytic conversion of ethanol into 1,3-butadiene on Cr-Ba/MCM-41 catalysts. *Brazilian J. Chem. Eng.* **2015**, *32*, 489–500. [CrossRef]

41. Corson, B.; Jones, H.; Welling, C.; Hinckley, J.; Stahly, E. Butadiene from ethyl alcohol. Catalysis in the one-and two-stop processes. *Ind. Eng. Chem.* **1950**, *42*, 359–373. [CrossRef]

42. Ohnishi, R.; Akimoto, T.; Tanabe, K. Pronounced catalytic activity and selectivity of MgO–SiO$_2$–Na$_2$O for synthesis of buta-1,3-diene from ethanol. *J. Chem. Soc., Chem. Commun.* **1985**, *70*, 1613–1614. [CrossRef]

43. Patel, A.D.; Meesters, K.; den Uil, H.; de Jong, E.; Blok, K.; Patel, M.K. Sustainability assessment of novel chemical processes at early stage: Application to biobased processes. *Energy Environ. Sci.* **2012**, *5*, 8430. [CrossRef]

44. Lewandowski, M.; Babu, G.S.; Vezzoli, M.; Jones, M.D.; Owen, R.E.; Mattia, D.; Plucinski, P.; Mikolajska, E.; Ochenduszko, A.; Apperley, D.C. Investigations into the conversion of ethanol to 1,3-butadiene using MgO:SiO$_2$ supported catalysts. *Catal. Commun.* **2014**, *49*, 25–28. [CrossRef]

45. Liu, P.; Hensen, E.J. M. Highly efficient and robust Au/MgCuCr$_2$O$_4$ catalyst for gas-phase oxidation of ethanol to acetaldehyde. *J. Am. Chem. Soc.* **2013**, *135*, 14032–14035. [CrossRef] [PubMed]

46. Bhattacharyya, S.K.; Avasthi, B.N. One-step catalytic conversion of ethanol to butadiene in a fluidized bed. *Ind. Eng. Chem. Process Des. Dev.* **1963**, *2*, 45–51. [CrossRef]

47. Kim, T.W.; Kim, J.W.; Kim, S.Y.; Chae, H.J.; Kim, J.R.; Jeong, S.Y.; Kim, C.U. Butadiene production from bioethanol and acetaldehyde over tantalum oxide-supported spherical silica catalysts for circulating fluidized bed. *Chem. Eng. J.* **2014**, *278*, 217–223. [CrossRef]

48. Quattlebaum, W.M.; Toussaint, W.J.; Dunn, J.T. Deoxygenation of certain aldehydes and ketones: preparation of butadiene and styrene. *J. Am. Chem. Soc.* **1947**, *1491*, 593–599. [CrossRef]

49. Sushkevich, V.L.; Palagin, D.; Ivanova, I.I. With open arms: Open sites of ZrBEA zeolite facilitate selective synthesis of butadiene from ethanol. *ACS Catal.* **2015**, *5*, 4833–4836. [CrossRef]

50. Angelici, C.; Meirer, F.; Van Der Eerden, A.M.J.; Schaink, H.L.; Goryachev, A.; Hofmann, J.P.; Hensen, E.J. M.; Weckhuysen, B.M.; Bruijnincx, P.C.A. Ex situ and operando studies on the role of copper in Cu-promoted SiO$_2$–MgO catalysts for the Lebedev ethanol-to-butadiene process. *ACS Catal.* **2015**, *5*, 6005–6015. [CrossRef]

51. Angelici, C.; Velthoen, M.E.Z.; Weckhuysen, B.M.; Bruijnincx, P.C.A. Influence of acid–base properties on the Lebedev ethanol-to-butadiene process catalyzed by SiO$_2$–MgO materials. *Catal. Sci. Technol.* **2015**, *5*, 2869–2879. [CrossRef]

52. Kvisle, S.; Aguero, A.; Sneeden, R.P.A. Transformation of ethanol into 1,3-butadiene over magnesium oxide/silica catalysts. *Appl. Catal.* **1988**, *43*, 117–131. [CrossRef]

53. Ordomskiy, V.V.; Sushkevich, V.L.; Ivanova, I.I. One-Step Method for Butadiene Production. U.S. Patent 8,921,635, 30 December 2014.

54. Ordomsky, V.V.; Sushkevich, V.L.; Ivanova, I.I. Study of acetaldehyde condensation chemistry over magnesia and zirconia supported on silica. *J. Mol. Catal. A* **2010**, *333*, 85–93. [CrossRef]

55. Sekiguchi, Y.; Akiyama, S.; Urakawa, W.; Koyama, T.R.; Miyaji, A.; Motokura, K.; Baba, T. One-step catalytic conversion of ethanol into 1,3-butadiene using zinc-containing talc. *Catal. Commun.* **2015**, *68*, 20–24. [CrossRef]

56. Simakova, O. A.; Davis, R.J.; Murzin, D.Y. *Biomass Processing over Gold Catalysts*; SpringerBriefs in Molecular Science; Springer International Publishing: Heidelberg, Germany, 2013.

57. Guan, Y.; Hensen, E.J.M. Ethanol dehydrogenation by gold catalysts: The effect of the gold particle size and the presence of oxygen. *Appl. Catal. A* **2009**, *361*, 49–56. [CrossRef]

58. Shimizu, K.I.; Sugino, K.; Sawabe, K.; Satsuma, A. Oxidant-free dehydrogenation of alcohols heterogeneously catalyzed by cooperation of silver clusters and acid-base sites on alumina. *Chem. -A Eur. J.* **2009**, *15*, 2341–2351. [CrossRef] [PubMed]

59. Sushkevich, V.L.; Ivanova, I.I.; Taarning, E. Mechanistic study of ethanol dehydrogenation over silica-supported silver. *ChemCatChem* **2013**, *5*, 2367–2373. [CrossRef]

60. Klein, A.; Keisers, K.; Palkovits, R. Formation of 1,3-butadiene from ethanol in a two-step process using modified zeolite-β catalysts. *Appl. Catal. A* **2015**, *1*, 192–202. [CrossRef]

61. Larina, O.V.; Kyriienko, P.I.; Soloviev, S.O. Effect of the addition of zirconium dioxide on the catalytic properties of ZnO/MgO-SiO$_2$ compositions in the production of 1,3-butadiene from ethanol. *Theor. Exp. Chem.* **2015**, *51*, 244–249. [CrossRef]

62. Kitayama, Y.; Michishita, A. Catalytic activity of fibrous clay mineral sepiolite for butadiene formation from ethanol. *J. Chem. Soc. Chem. Commun.* **1981**, *9*, 401–402. [CrossRef]

63. Kitayama, Y.; Satoh, M.; Kodama, T. Preparation of large surface area nickel magnesium silicate and its catalytic activity for conversion of ethanol into buta-1,3-diene. *Catal. Lett.* **1996**, *36*, 95–97. [CrossRef]

64. Kitayama, Y.; Shimizu, K.; Kodama, T.; Murai, S.; Mizusima, T.; Hayakawa, M.; Muraoka, M. Role of intracrystalline tunnels of sepiolite for catalytic activity. *Stud. Surf. Sci. Catal.* **2002**, *142*, 675–682.

65. Parr, R.G.; Pearson, R.G. Absolute hardness: Companion parameter to absolute electronegativity. *J. Am. Chem. Soc.* **1983**, *105*, 7512–7516. [CrossRef]

66. Yang, W.; Parr, R.G. Hardness, softness, and the fukui function in the electronic theory of metals and catalysis. *Proc. Natl. Acad. Sci.* **1985**, *82*, 6723–6726. [CrossRef] [PubMed]

67. Toussaint, W.J.; Dunn, J.T.; Jackson, D.R. Production of butadiene from alcohol. *Ind. Eng. Chem.* **1947**, *39*, 120–125. [CrossRef]

68. Sushkevich, V.L.; Ivanova, I.I.; Tolborg, S.; Taarning, E. Meerwein-Ponndorf-Verley-Oppenauer reaction of crotonaldehyde with ethanol over Zr-containing catalysts. *J. Catal.* **2014**, *316*, 121–129. [CrossRef]

69. Sushkevich, V.L.; Ivanova, I.I.; Taarning, E. Ethanol conversion into butadiene over Zr-containing molecular sieves doped with silver. *Green Chem.* **2015**, *17*, 2552–2559. [CrossRef]

70. Sushkevich, V.L.; Vimont, A.; Travert, A.; Ivanova, I.I. Spectroscopic evidence for open and closed Lewis acid sites in ZrBEA zeolites spectroscopic evidence for open and closed Lewis acid sites in ZrBEA zeolites. *J. Phys. Chem. C* **2015**, *119*, 17633–17639. [CrossRef]

71. Courtney, T.D.; Chang, C.; Gorte, R.J.; Lobo, R.F.; Fan, W.; Nikolakis, V. Microporous and mesoporous materials effect of water treatment on Sn-BEA zeolite: Origin of 960 cm$^{-1}$ FTIR peak. *Microporous Mesoporous Mater.* **2015**, *210*, 69–76. [CrossRef]

72. Ratnasamy, P.; Srinivas, D.; Knözinger, H. Active sites and reactive intermediates in titanium silicate molecular sieves. *Adv. Catal.* **2004**, *48*, 1–169. [CrossRef]

73. Boronat, M.; Concepción, P.; Corma, A.; Renz, M.; Valencia, S. Determination of the catalytically active oxidation Lewis acid sites in Sn-beta zeolites, and their optimisation by the combination of theoretical and experimental studies. *J. Catal.* **2005**, *234*, 111–118. [CrossRef]

74. Boronat, M.; Concepción, P.; Corma, A.; Navarro, M.T.; Renz, M.; Valencia, S. Reactivity in the confined spaces of zeolites: The interplay between spectroscopy and theory to develop structure–activity relationships for catalysis. *Phys. Chem. Chem. Phys.* **2009**, *11*, 2876–2884. [CrossRef] [PubMed]

75. Harris, J.W.; Cordon, M.J.; Di Iorio, J.R.; Vega-vila, J.C.; Ribeiro, F.H.; Gounder, R. Titration and quantification of open and closed Lewis acid sites in Sn-Beta zeolites that catalyze glucose isomerization. *J. Catal.* **2016**, *335*, 141–154. [CrossRef]

76. Zhu, Y.; Chuah, G.; Jaenicke, S. Chemo- and regioselective Meerwein-Ponndorf-Verley and Oppenauer reactions catalyzed by Al-free Zr-zeolite beta. *J. Catal.* **2004**, *227*, 1–10. [CrossRef]

77. Sun, J.; Zhu, K.; Gao, F.; Wang, C.; Liu, J.; Peden, C.H.F.; Wang, Y. Direct conversion of bio-ethanol to isobutene on nanosized $Zn_xZr_yO_z$ mixed oxides with balanced acid-base sites. *J. Am. Chem. Soc.* **2011**, *133*, 11096–11099. [CrossRef] [PubMed]

78. Liu, J.Y.; Su, W.N.; Rick, J.; Yang, S.C.; Cheng, J.H.; Pan, C.J.; Lee, J.F.; Hwang, B.J. Hierarchical copper-decorated nickel nanocatalysts supported on $La_2O_3$ for low-temperature steam reforming of ethanol. *ChemSusChem* **2014**, *7*, 570–576. [CrossRef] [PubMed]

79. Frey, A.M.; Karmee, S.K.; de Jong, K.P.; Bitter, J.H.; Hanefeld, U. Supported $La_2O_3$ and MgO nanoparticles as solid base catalysts for aldol reactions while suppressing dehydration at room temperature. *ChemCatChem* **2013**, *5*, 594–600. [CrossRef]

80. Boukha, Z.; Fitian, L.; López-Haro, M.; Mora, M.; Ruiz, J.R.; Jiménez-Sanchidrián, C.; Blanco, G.; Calvino, J.J.; Cifredo, G.A.; Trasobares, S.; et al. Influence of the calcination temperature on the nano-structural properties, surface basicity, and catalytic behavior of alumina-supported lanthana samples. *J. Catal.* **2010**, *272*, 121–130. [CrossRef]

81. Kozlowski, J.T.; Davis, R.J. Sodium modification of zirconia catalysts for ethanol coupling to 1-butanol. *J. Energy Chem.* **2013**, *22*, 58–64. [CrossRef]

82. Han, Y.; Lee, S.S.; Ying, J.Y. Spherical siliceous mesocellular foam particles for high-speed size exclusion chromatography. *Chem. Mater.* **2007**, *19*, 2292–2298. [CrossRef]

83. Legendre, M.; Cornet, D. Catalytic oxidation of ethanol over tantalum oxide. *J. Catal.* **1972**, *25*, 194–203. [CrossRef]

84. Tanabe, K. Catalytic application of niobium compounds. *Catal. Today* **2003**, *78*, 65–77. [CrossRef]

85. Jehng, J.M.; Wachs, I.E. The molecular structures and reactivity of supported niobium oxide catalysts. *Catal. Today* **1990**, *8*, 37–55. [CrossRef]

86. Jehng, J.-M.; Wachs, I.E. Molecular structures of supported niobium oxide catalysts under ambient conditions. *J. Mol. Catal.* **1991**, *67*, 369–387. [CrossRef]

87. Kosslick, H.; Lischke, G.; Parlitz, B.; Storek, W.; Fricke, R. Acidity and active sites of Al-MCM-41. *Appl. Catal. A* **1999**, *184*, 49–60. [CrossRef]

88. Aimon, D.; Panier, E. La mise en pratique de l'économie circulaire chez Michelin. *Ann. des Mines-Responsab. Environ.* **2014**. [CrossRef]